The Institute of Paper Chemistry

Appleton, Wisconsin

Doctor's Dissertation

An Investigation of the Mechanism of the Dewatering of Compressible Beds

Robert W. Hisey

June, 1955

AN INVESTIGATION OF THE MECHANISM OF THE DEWATERING OF COMPRESSIBLE BEDS

A thesis submitted by

Robert W. Hisey

B.A. 1952, Middlebury College
M.S. 1954, Lawrence College

in partial fulfillment of the requirements
of The Institute of Paper Chemistry
for the degree of Doctor of Philosophy
from Lawrence College,
Appleton, Wisconsin

June, 1955

TABLE OF CONTENTS

INTRODUCTION

The removal of water or other fluids from suspensions of solid materials by the application of pressure is an important operation in many industries. The paper industry is one of these, and is concerned with this type of dewatering in all its draining, washing, pressing, and sheet-forming operations (see Appendix I).

There are several separate stages which are distinguishable in this over-all process of dewatering; these have different mechanisms. These stages may be recognized from an examination of the one-dimensional dewatering of slurries of two types of materials. The first type of material is that which forms relatively incompressible beds, for example, sand, glass beads, and calcium carbonate. The second type of material is that which forms compressible beds, for example, papermaking fibers, glass wool, and most commercial sludges.

The first case to be examined is the one-dimensional dewatering of a slurry of a material which forms an incompressible bed. The first stage of dewatering would be a conventional filtration operation. Consider a slurry of this material in a tube with a permeable septum on the bottom. As water is removed from the slurry through the septum, a pad of material is built up on the septum. The amount of free slurry above the pad steadily decreases. The pad formed is isotropic and the weight of solids in the bed is usually linearly related to the volume of filtrate. The filtration rate in this case is exactly expressed by a modification of D'Arcy's law (1).

This initial stage of dewatering comes to an end when there is no free slurry left above the pad. That is, the top level of the free slurry coincides with the top level of the pad. All of the solids which were originally present in the slurry are now immobilized in the bed, unless any have passed through the septum. On continuing to drain water through the septum, the final stage of dewatering is entered. In this stage, no new solids are added to the pad. Since there is no slurry above the pad, the water removed must come out of the pad itself. However, the pad is incompressible, and so the water must leave the bed capillaries and be replaced by air. This stage of dewatering has been recognized by a number of workers and some fundamental concepts have been clarified (2, 3, 4).

The second case to be considered is the one-dimensional dewatering of a slurry of a material which forms a compressible bed. In this case, the dewatering may be divided into three stages, instead of two as in the case of incompressible materials. Consider a slurry of the compressible material in a tube with a septum on the bottom. As water is drained through the septum, the three separate stages succeed one another.

The first stage is a true filtration, and a mat is built up on the septum just as in the case of incompressible materials. However, the mat formed is nonuniform because of the greater compression of the lower elements of the pad from the frictional pressure drop across the higher elements, since the compressive stress at a point is equal to the pressure drop to that point. It has a density and porosity gradient of the pad solids from the bottom of the pad to the top. The filtration behavior of slurries of this type has been elucidated on the basis of an integrated form of D'Arcy's law, which allows for the variation in filtration

resistance within the pad (5, 6, 7, 8). This stage ends when the free liquid surface contacts the top surface of the pad.

The second, or intermediate stage of dewatering, which will be called thickening, begins just as the last of the free slurry disappears, and only bed is left in the tube. The water which continues to drain through the septum must now be coming from within the pad, and not through it as in the first filtration stage. Since the pad is compressible, water is now squeezed out of the pad, without the introduction of air.

Thus, the pad is being compressed, which means that there must be a steadily increasing compressive stress exerted on the top layer of particles in the bed. This force is supplied, in this case, by the surface-tension pressures of the water in the capillaries at the pad surface. However, at some later time, the surface-tension pressures may be exceeded in the larger capillaries, and these capillaries will start to drain, ending the thickening stage.

The last stage of this dewatering, that of the displacement of part of the water in the interior of the pad with a second fluid such as air, begins when air first enters the pad. The mechanism of this stage, while mathematically very complicated, should be closely analogous to the corresponding stage in the dewatering of incompressible materials.

The intermediate or thickening stage, which is the subject of this work, has not been clearly recognized, either in the literature or in the paper industry. A search of the literature reveals some workers who have apparently commented upon this phenomenon, or at least some phase of it.

Preston and Nimkar (9) and Christensen and Barkas (10) recognized that when water is drained from a wet pad of compressible material there is a contraction of the pad under the influence of surface-tension pressures, and that there may be an eventual equilibrium established when the hydrostatic tension is balanced by the elastic forces in the pad. However, they do not extend their work beyond this observation.

Campbell (11) recognized a "removal of water by compaction" in the latter stages of sheet formation on a fourdrinier wire, which may be the regime of thickening. However, his treatment of the phenomenon is rather oversimplified. He considered the process to be one of permeation with a mean effective path for the water travel of one half of the total pad thickness. He also assumed that there is a uniform compacting rate throughout the pad, and that none of the compacting load is carried by the pad. This treatment is considered not complete, if it was meant to apply to the same process discussed here as thickening.

Cowan (12) postulated that even on the first part of the fourdrinier wire there is no pad formation, but that there is a smooth concentration gradient from the wire to the top of the slurry. For drainage near the suction boxes he assumed that the mechanism was that of permeation. This assumption led to a rather simple expression for drainage rates in what may be the regime of thickening, but seems somewhat oversimplified.

Ingmanson and Whitney (8) first made use of the term thickening in connection with this phenomenon. They stated that in the dewatering of pulp slurries of over about 2% fiber by weight there is no sharp line of demarcation between the pad and the slurry. They have calculated that this

is the minimum fiber concentration under their conditions which had mechanical strength under compressive load. However, they do not consider the mechanism of water removal in this thickening except to indicate that it is different from the customary filtration or permeation cases.

POSTULATED MECHANISM OF THICKENING

The term thickening as used in this work will refer to the removal of fluid from a continuous bed of a compressible material by the one-dimensional compression of the bed under an applied load. This is to occur without the entry of a second fluid into the bed. It is of no consequence whether this compressibility is caused by an elasticity of the particles and bed or by the irreversible deflocculation of the bed by applied pressure as discussed by Grace (13). The flocs, however, must be small in comparison to the bed itself.

There are certain observations which may be made from an inductive analysis of the operation. The first observation is that the bed is composed of a continuous fluid network under fluid load and a continuous solid network under mechanical load. That is, all of the solid elements of the bed are supporting a compressive stress. The second observation is that the fluid movement is out of the bed rather than through the bed as in filtration and permeation. As a consequence, the flow rate, the mechanical stress, and the fluid pressure are not constant throughout the bed.

The third observation is that for a given constant pressure drop across the bed there may be an equilibrium condition where the pressure is entirely supported by the mechanical strength of the bed, and flow and compression cease. This would be the end of a constant-pressure thickening, and has been observed by Preston and Nimkar (9) and Christensen and Barkas (10), as previously noted. The fourth observation, a corollary of the

third, is that the entire pressure applied across the pad during thickening is not available as a driving force for fluid flow. On the contrary, it is seen that as the thickening proceeds more and more of the applied pressure is counteracted by the mechanical strength of the bed.

The fifth observation is that the mechanical stress on any solid element of the bed is transmitted directly to the solid element below it, augmented by the frictional pressure drop in the fluid moving across the element. That is, the change in mechanical stress as one moves through the bed is numerically equal to the change in fluid driving force, but of opposite sign. From this it follows that at any point in the bed the sum of the mechanical stress on the solid element and the fluid driving force is equal to the total effective pressure drop across the pad. From these observations one may proceed to the derivation of a mathematical expression relating the flow rate, pad properties, applied pressure, and time.

The usual basic equation of filtration and permeation work is a modified form of D'Arcy's law, which is based upon a simplified form of the Poiseuille equation, and is thus confined to laminar flow (1). For the whole pad, this equation may be written as*

$$\underline{q} = (\underline{A}\Delta\underline{P}_f)/(\mu\underline{R}_t), \qquad (1)$$

where $\underline{q}$ is the flow rate of an incompressible fluid of viscosity μ flowing under a driving force equal to $\Delta\underline{P}_f$ through a pad of cross-section $\underline{A}$. $\underline{R}_t$ is the total resistance of the bed for unit cross-sectional area. This resistance may be expressed as specific resistance on a mass basis. Equation (1) may then be written for the whole pad, whether of compressible

---

* All symbols are defined in Table I. All pressures are corrected to the same datum plane.

or incompressible material, as

$$q = (A\Delta P_f)/(\mu M R_{av}), \qquad (2)$$

where M is the total mass per unit area of the bed, and R_{av} is the average specific resistance of the bed. This equation may now be written in a differential form for a differential element of m, the mass per unit area of the bed from the top surface down to any point.

$$q = (A\, d\Delta P_f)/(\mu R\, dm) \qquad (3)$$

R is the point specific resistance of the bed. These considerations assume that the contraction and expansion losses as the fluid enters or leaves the bed are negligible. With the low velocities used, this is true, the maximum effect being only a few dynes per sq. cm.

Consider now a bed in the process of thickening as shown in Figure 1, with the fluid flowing out of the bottom only. Let ΔP be the total pressure drop across the pad at time θ, m the mass per unit area of the pad from the surface down to the point m, P_S the mechanical compressive stress at that point, and P_L the hydrostatic pressure in the fluid at that point available as a driving force for fluid flow. That is, it is the difference in static pressure between that point and the septum corrected to the same datum plane. P_{so} is the mechanical compacting force born by the uppermost element of the solid. From these definitions and the previous observations, the pressure relationships shown in Figure 1 may be written assuming that the net weight of the fibers in water exerts a negligible compressive stress.

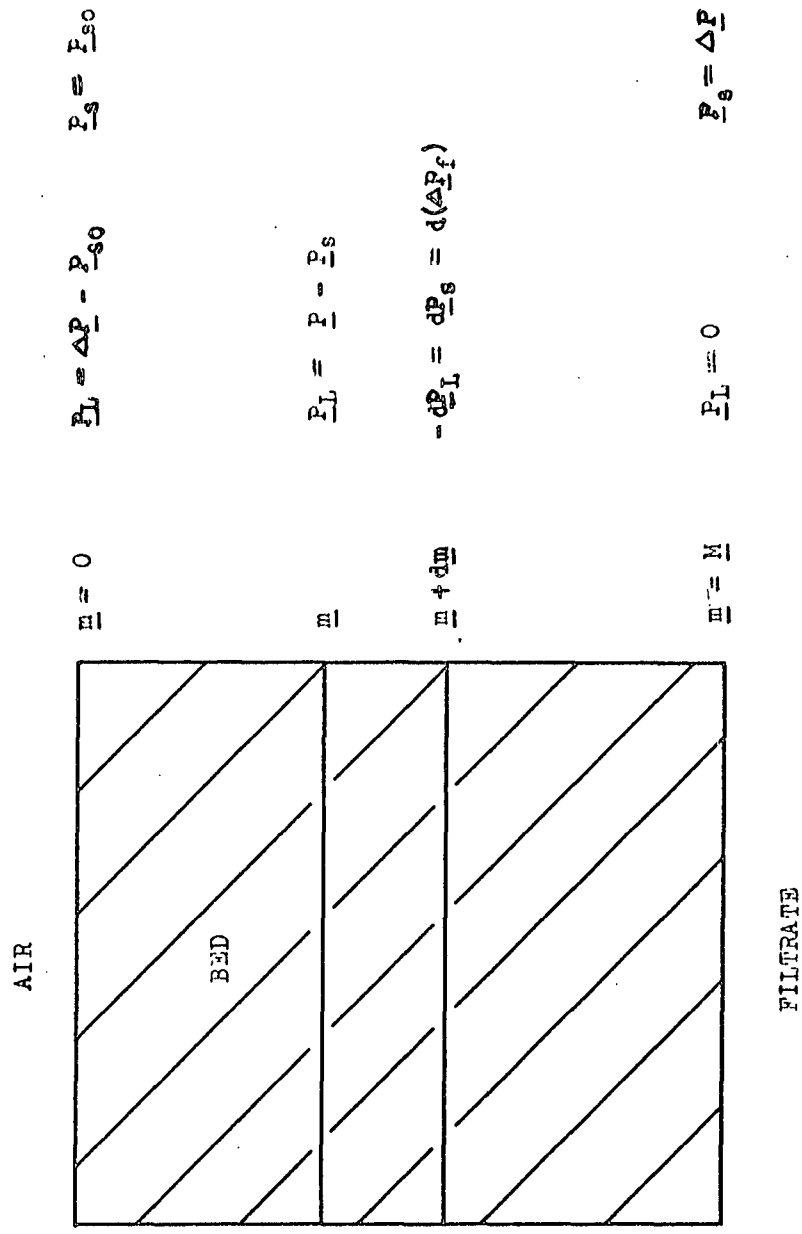

Figure 1 Diagram of Bed Undergoing Thickening

TABLE I

NOMENCLATURE

(In consistent c.g.s. units)

A	Cross-sectional area of bed, 50 sq. cm. for septum.
B	A parameter, $\alpha M^2 q_M / V_o$, dyne g. ^{2}/cm.^{6}
c	Concentration of bed, dry solids, g./cc.
c_s	Mass of fiber in filter bed per unit volume of filtrate, g./cc.
g	Acceleration due to gravity, 980 cm./sec./sec.
h	Pad height, cm.
k	Corrected permeability, g./cm.
M	Total mass of bed per unit area, g./sq. cm.
M'	Mass fraction of bed per unit area down to a point m, dimensionless.
m	Mass of bed per unit area down to a point m, g./sq. cm.
P_L	Fluid driving force, dynes/sq. cm.
P_s	Mechanical compacting pressure, dynes/sq. cm.
P_{so}	Compacting force at the top face of the bed, dynes/sq. cm.
ΔP	Total pressure drop across bed, dynes/sq. cm.
ΔP_f	Total frictional pressure drop across bed, dynes/sq. cm.
ΔP_o	Total pressure drop across bed at start of thickening, dynes/sq. cm.
q	Flow rate, cc./sec.
R	Point specific resistance of bed for unit area, mass basis, cm./g.
R_{av}	Average specific resistance of bed for unit area, mass basis, cm./g.
R_t	Total resistance of bed for unit area, 1/cm.
V	Volume of bed, cc.
V_o	Volume of bed at start of thickening, cc.

TABLE I (Continued)

$\underline{V}'$	Instantaneous internal pad volume fraction, dimensionless.
$\underline{v}$	Total pad volume fraction of original pad volume, $\underline{V}/\underline{V}_o$, dimensionless.
$\underline{Y}$	Point compressibility of bed, cm. ^{5}/g. dyne.
μ	Viscosity of filtrate, poises.
θ	Time from start of thickening, seconds.
ρ	Density of filtrate, g./cc.
τ	Corrected pressure, dynes/sq. cm.
τ_o	Corrected pressure at the top face of pad, dynes/sq. cm.
$\Delta\tau$	Over-all corrected pressure drop across pad, dynes/sq. cm.
$\Delta\tau_o$	Original over-all corrected pressure drop across pad at start of thickening, dynes/sq. cm.

Consider now the element of mass per unit area $d\underline{m}$ between the points $\underline{m}$ and $\underline{m} + d\underline{m}$. For the flow into this element from above, one may write, from Equation (3) and the pressure relationships in Figure 1:

$$\underline{q}_m = - (\underline{A}/\underline{R}\mu)(\partial \underline{P}_L/\partial \underline{m}), \tag{4}$$

where $\underline{q}_m$ is the instantaneous flow rate at the point $\underline{m}$. At the same instant, the flow out of this element from $\underline{m} + d\underline{m}$ is given by

$$\underline{q}_{m + dm} = -(\underline{A}/\underline{R}\mu)(\partial \underline{P}_L/\partial \underline{m}) + (\partial/\partial \underline{m})[-(\underline{A}/\underline{R}\mu)(\partial \underline{P}_L/\partial \underline{m})]d\underline{m}. \tag{5}$$

Thus, the net flow out of the element is the difference between the gain as expressed by Equation (4) and the loss as expressed by Equation (5). This net rate is

$$d\underline{q} = (\partial/\partial \underline{m})[-(\underline{A}/\underline{R}\mu)(\partial \underline{P}_L/\partial \underline{m})]d\underline{m}. \tag{6}$$

But the net flow out of the element is the depletion, or the rate of volumetric contraction of the mass element. This may also be expressed as

$$d\underline{q} = -\underline{A}[\partial(1/\underline{c})/\partial\theta]d\underline{m}, \tag{7}$$

where $(1/\underline{c})$ is the total volume associated with a unit mass of fiber at a point concentration $\underline{c}$, and $d\underline{q}$ is the net flow increment across $d\underline{m}$ at time θ. Equations (6) and (7) may be combined to give

$$\partial(1/\underline{c})/\partial\theta = (\partial/\partial \underline{m})[(1/\underline{R}\mu)(\partial \underline{P}_L/\partial \underline{m})]. \tag{8}$$

Now let $\underline{Y}$ be the point compressibility of the pad on a mass basis. That is, $\underline{Y}$ is defined as the rate of change with applied mechanical pressure of the volume of water plus fiber associated with a unit mass of fiber.

Therefore, assuming $(1/\underline{c})$ to be a function of $\underline{P}_s$ only, $\underline{Y}=d(1/\underline{c})/d\underline{P}_s$, where $\underline{c}$ is the point concentration of solid material in the bed by weight at a compacting pressure $\underline{P}_s$. However, this may be writted as $d(1/\underline{c})=\underline{Y}\ d\underline{P}_s$, and the term $d\underline{P}_s$ expanded to give

$$d(1/\underline{c}) = \underline{Y}\ d\underline{P}_s = \underline{Y}(\partial \underline{P}_s/\partial \underline{m})\ d\underline{m} + \underline{Y}(\partial \underline{P}_s/\partial \theta)\ d\theta. \tag{9}$$

Identifying terms gives

$$\partial(1/\underline{c})/\partial\theta = \underline{Y}(\partial \underline{P}_s/\partial\theta). \tag{10}$$

Combining Equations (8) and (10) gives

$$\underline{Y}(\partial \underline{P}_s/\partial\theta) = (\partial/\partial \underline{m})[(1/\underline{R}\mu)(\partial \underline{P}_L/\partial \underline{m})]. \tag{11}$$

But from the pressure relationships in Figure 1, it is seen that

$$\underline{P}_s = \Delta \underline{P} - \underline{P}_L \tag{12}$$

and from this

$$\partial \underline{P}_s/\partial \underline{m} = -\partial \underline{P}_L/\partial \underline{m}. \tag{13}$$

Combining Equations (11) and (13) gives

$$\underline{Y}(\partial \underline{P}_s/\partial\theta) = -(\partial/\partial \underline{m})[(1/\underline{R}\mu)(\partial \underline{P}_s/\partial \underline{m})]. \tag{14}$$

This equation should describe the course of any thickening operation. However, in this form it is intractable. In order to simplify the equation, the dependent variable $\underline{P}_s$ may now be transformed to a new variable γ, as has been suggested by Plunkett (14) in the treatment of unsteady state heat conduction. This new variable still retains the units of pressure, and is

defined by the equation

$$d\underline{P}_s/\underline{R} = \underline{k}\, d\,\tau, \tag{15}$$

where $\underline{k}$ is defined as a constant with the units of reciprocal filtration resistance. That is, it has the units of a permeability coefficient on a mass basis. Since it has been assumed that $\underline{R}$ is a function of $\underline{P}_s$ only, and not of $\underline{m}$ or θ, the differentials in Equation (15) may be expanded to give

$$(1/\underline{R})[(\partial\underline{P}_s/\partial\theta)\, d\theta + (\partial\underline{P}_s/\partial\underline{m})\, d\underline{m}] = \underline{k}[\partial\tau/\partial\theta)\, d\theta + (\partial\tau/\partial\underline{m})\, d\underline{m}] \tag{16}$$

Solving Equation (16) for the appropriate quantities and substituting into Equation (14) gives

$$\underline{Y}\underline{k}\underline{R}(\partial\tau/\partial\theta) = -(\partial/\partial\underline{m})[(1/\underline{R}\mu)\underline{k}\underline{R}(\partial\tau/\partial\underline{m})]. \tag{17}$$

From this it follows that

$$\mu\underline{Y}\underline{R}(\partial\tau/\partial\theta) = -\partial^2\tau/\partial\underline{m}^2. \tag{18}$$

This equation is simply Equation (14) expressed in transformed pressure units. In Equation (14) it may be seen that $\underline{Y}$ and $\underline{R}$, the two functions of $\underline{P}_s$, may not be combined into a single term. In the transformed equation (18), on the other hand, they may be, giving the one term $\underline{Y}\underline{R}$. This facilitates the handling of the equation and the attainment of numerical solutions.

To evaluate τ and $\underline{k}$, τ is set numerically equal to $\underline{P}_s$ at the extreme limits of interest in the particular system. This is an arbitrary choice dictated merely by convenience. It is necessary to impose two arbitrary

conditions in order to establish the size of the τ units and their absolute magnitude. These limits are

$$\tau_1 = \underline{P}_{s_1} \qquad \text{and} \qquad \tau_2 = \underline{P}_{s_2} \tag{19}$$

Using these boundaries to integrate Equation (15) and rearranging the resultant integrals, one may obtain

$$\underline{k} = [1/(\tau_1 - \tau_2)] \int_{\underline{P}_{s_1}}^{\underline{P}_{s_2}} d\underline{P}_s/\underline{R} \tag{20}$$

and

$$\tau = \tau_1 + (1/\underline{k}) \int_{\underline{P}_{s_1}}^{\underline{P}_s} d\underline{P}_s/\underline{R}. \tag{21}$$

In Equation (18), supplemented by Equations (19), (20), and (21), there are now present tractable general expressions from which the entire course of a one-dimensional thickening should be predictable. This prediction would entail only a knowledge of the properties $\underline{R}$ and $\underline{c}$ as functions of $\underline{P}_s$ of the compressible material and of the particular boundary conditions peculiar to each thickening.

CONSTANT-RATE THICKENING

While Equation (18) is a general form, it may be further simplified for certain conditions of restraint such as occur in constant-rate thickenings, where the over-all rate of water removal from the bed is held constant throughout the course of the thickening. This will be shown.

A reduced mass-per-unit-area term M' is defined as

$$\underline{M}' = \underline{m}/\underline{M}. \tag{22}$$

Then the right side of Equation (18) is evaluated in terms of this new variable.

$$\partial^2\psi/\partial\underline{m}^2 = (1/\underline{M}^2)(\partial^2\psi/\partial\underline{M}'^2) \tag{23}$$

Now a reduced total pad volume $\underline{v}$ is introduced, such that

$$\underline{v} = \underline{V}/\underline{V}_o, \tag{24}$$

where $\underline{V}$ is the total volume of the pad at the time θ and $\underline{V}_o$ is the total volume of the pad when $\theta = 0$. But, since the volume rate of flow out of the pad is constant, then

$$\underline{V} = \underline{V}_o - \theta\underline{q}_M, \tag{25}$$

where $\underline{q}_M$ is the volumetric flow rate at mass point $\underline{M}$, which is the flow rate out of the pad. Then Equations (24) and (25) combine to give

$$(1 - \underline{v}) = \theta\underline{q}_M/\underline{V}_o. \tag{26}$$

Then the left side of Equation (18) is evaluated with the help of Equation (26) to give in terms of the new variable

$$\underline{Y}\underline{R}\mu(\partial\psi/\partial\theta) = \underline{Y}\underline{R}\mu[\partial\psi/\partial(1 - \underline{v})][\partial(1 - \underline{v})/\partial\theta] =$$

$$(\underline{Y}\underline{R}\mu\underline{q}_M/\underline{V}_o)[\partial\psi/\partial(1 - \underline{v})]. \tag{27}$$

Equations (23) and (27) are now substituted into Equation (18) to give

$$-(1/\underline{M}^2)(\partial^2\psi/\partial\underline{M}'^2) = (\underline{Y}\underline{R}\mu\underline{q}_M/\underline{V}_o)[\partial\psi/\partial(1 - \underline{v})], \tag{28}$$

which upon rearrangement becomes

$$-\partial^2\psi/\partial\underline{M}'^2 = (\underline{M}^2\underline{Y}\underline{R}\mu\underline{q}_M/\underline{V}_o)[\partial\psi/\partial(1 - \underline{v})]. \tag{28a}$$

Now one may impose another condition of restraint and specify that the original condition of the pad before thickening commences is that of permeation at the same constant flow rate as that at which the thickening is carried out. Now, $\underline{M}$, $\underline{V}_o$, and $\underline{q}_M$ may be interrelated. Equation (2), which applies to the whole pad while undergoing permeation, may be rearranged to give

$$\underline{M}\mu\underline{q}_M = \underline{A}\Delta\underline{P}_f/\underline{R}_{av}. \tag{29}$$

The total volume of the pad while undergoing permeation, and thus also at the start of thickening, is seen to be

$$\underline{V}_o = \underline{A}\int_0^{\underline{M}} d\underline{m}/\underline{c} \tag{30}$$

But Equations (2) and (3) may be combined and rearranged to give

$$d\underline{m} = \underline{M}\underline{R}_{av}\, d\Delta\underline{P}_f/\Delta\underline{P}_f\underline{R}, \tag{31}$$

which may be combined with Equation (30) to give

$$\underline{V}_o/\underline{M} = (\underline{A}\underline{R}_{av}/\Delta\underline{P}_f)\int_0^{\Delta\underline{P}_f} d\Delta\underline{P}_f/\underline{c}\underline{R}. \tag{32}$$

Equation (29) may now be divided by Equation (32) to give

$$\mu\underline{M}^2\underline{q}_M/\underline{V}_o = [(\Delta\underline{P}_f)^2/\underline{R}^2_{av}]/\int_0^{\Delta\underline{P}_f} d\Delta\underline{P}_f/\underline{c}\underline{R} = \underline{B} \tag{33}$$

and it is seen that, for a given material, $\underline{B}$ is a function only of the original frictional pressure drop across the pad. Substituting $\underline{B}$ into Equation (28a) gives a final reduced form.

$$-\partial^2\gamma/\partial\underline{M}'^2 = \underline{B}\underline{Y}\underline{R}\,\partial\gamma/\partial(1 - \underline{v}) \tag{34}$$

It will be recalled that τ is a reduced pressure, $\underline{M}'$ a reduced mass per unit area, $\underline{Y}$ the point compressibility of the pad, $\underline{R}$ the point specific resistance of the pad, $\underline{B}$ a function only of the material and the original pressure drop across the pad, and $(1-\underline{v})$ the volume fraction of the bed removed or pad volume contraction, which is essentially a reduced time measurement.

Thus, it is evident that for a given material the differential equations for all constant-rate thickenings proceeding from permeations are all identical, providing only that the original over-all pressure drops are the same. For the solutions of the equations to be identical, however, it is further necessary that the two boundary conditions be identical. This is easily shown. One of these boundary conditions is the original τ distribution within the pad as a function of $\underline{M}'$. During permeation, the flow rate is constant throughout the pad, and from Equations (3), (12), and (15), may be written

$$\underline{q} = (\underline{A}/\mu)(d\Delta P_f/\underline{R}\, d\underline{m}) = (\underline{Ak}/\mu)(d\tau/d\underline{m}), \tag{35}$$

for a point in the pad. Integrating across the whole pad gives

$$\underline{q} = \underline{Ak}\Delta\tau_o/\underline{M}\mu. \tag{36}$$

Combining Equations (35) and (36), integrating, and substituting $\underline{M}'$ from Equation (22) gives

$$\tau = \tau_o + \int_0^{\underline{m}} (\Delta\tau_o/\underline{M})d\underline{m} = \tau_o + \underline{M}'\Delta\tau_o. \tag{37}$$

Thus, it may be seen that the τ distribution in a pad undergoing permeation, and thus also at the start of thickening in this case, is linear with $\underline{M}'$, and is dependent only on the total pressure drop across the pad.

The other boundary condition in the case under consideration is the tau gradient at the septum. Since the flow rate at the septum is constant throughout the course of the thickening, Equation (35) may be rearranged to give

$$\underline{M}(\partial\tau/\partial\underline{m})_{M} = (\underline{M}\mu\underline{q}_{M}/\underline{Ak}) = (\partial\tau/\partial\underline{M}')_{M' = 1}, \tag{38}$$

but from Equation (36)

$$\underline{M}\mu\underline{q}_{M}/\underline{Ak} = \Delta\tau_{o}. \tag{39}$$

Combining Equations (38) and (39) gives

$$(\partial\tau/\partial\underline{M}')_{M' = 1} = \Delta\tau_{o}. \tag{40}$$

Thus, it may be seen that the tau gradient with respect to $\underline{M}'$ at the septum is constant during the course of a constant-rate thickening, and its value is dependent only on the initial pressure drop across the pad.

Since both the boundary conditions and the differential equations are identical for all constant-rate thickenings which are continuations of permeations, and which have the same initial over-all pressure drop at the onset of thickening, the solutions of the equations (in terms of tau; $\underline{M}'$ and $(1-\underline{v})$ must be identical, for a given material.

An analytical solution of Equation (34) was not found. Solutions may be obtained by a standard iterative technique described by Plunkett (14), among others.

METHOD OF ATTACK

Up to this point in the work, a general equation for the one-dimensional case of the postulated thickening operation has been developed. For the special case of a constant-rate thickening proceeding from a permeation at the same rate, further simplification of the equation was seen to be possible.

In order to test the theory, thickenings were to be conducted and the observed results compared with the predicted results. There are a number of possible pressure or rate schedules which could be used in these tests, but the two most commonly encountered in the field of filtration and permeation are constant rate of fluid extraction and constant applied pressure. These are not the only schedules of commercial importance, but they are the easiest to treat mathematically and are as valid tests of general theory as any other schedules.

It was found that the apparatus built was more precise and convenient when operated on a constant-rate schedule than on a constant-pressure schedule. This, coupled with the fact that certain simplifications in the mathematics for this case were possible which cut down the number of numerical iterative solutions necessary, is the reason that it was decided to test the general theory by its application to the case of constant-rate thickenings of beds which had been permeated at the same rate. This testing does not limit the applicability or generality of the primary theory and equations.

In the discussion and derivations, the more complicated case was presented, where the compressive stress at the pad surface is supplied by

the surface tension pressures. However, this should not be thought a necessary condition for thickening, as this force may be applied in any manner. In the experimental work, it was found desirable to apply this force by means of an impermeable piston, which effectively compresses the bed. This was necessary, for if surface tension pressures are relied upon and a small area of bed is used, the top of the bed may shrink appreciably in the area under the influence of forces arising from the surface tension of the fluid. This would mean that the thickening would no longer be even a close approximation to the presupposed one-dimensional case.

Previous work in filtration and fluid flow has indicated that the only effect of temperature in fluid flow through porous beds is on the viscosity of the fluid, aside from density considerations. For this reason, it was felt permissible to eliminate temperature as a variable for study, and so all runs were made over a narrow range of temperature.

EXPERIMENTAL APPARATUS

An experimental apparatus was built which was similar to that used by Ingmanson (5, 8). This apparatus was designed so as to permit the carrying out of constant-rate filtrations at dilute pre-filt concentrations, the carrying out of thickening runs, and the determination of pulp compressibilities. The major features of the apparatus are shown in Figures 2 and 3.

Figure 2 is a drawing of the filtration- or thickening-tube assembly itself. The filtration tube was made of 3/16-in.-wall methyl methacrylate (Lucite) tubing to provide for visual observation. The tube had a nominal 3-1/8-in. I. D. (internal diameter), and an actual cross-sectional area of exactly 50 sq. cm. There were nine pressure taps set into the side wall of the tube near the bottom. These taps were 3/16-in. I. D., 5/16-in. O. D. (outside diameter) Lucite tubes placed on 1-cm. centers vertically and staggered around one-third of the tube horizontally. The fourth and fifth taps from the bottom were the same height above the bottom of the tube but displaced horizontally one-third of the way around the tube.

In the top of the tube a 1/16-in. shoulder was cut down 1/2 in. into the tube to facilitate the entry of the piston. To the top of the tube was glued a 5-7/8-in. flange of one-inch Lucite to provide for attaching the head tube and base.

The head tube was a four-inch section of 5-7/8-in. I. D., 6-1/8-in. O. D. Lucite tubing glued to a bottom of one-inch sheet Lucite. The bottom was cut out to match the filtration tube's internal diameter. At

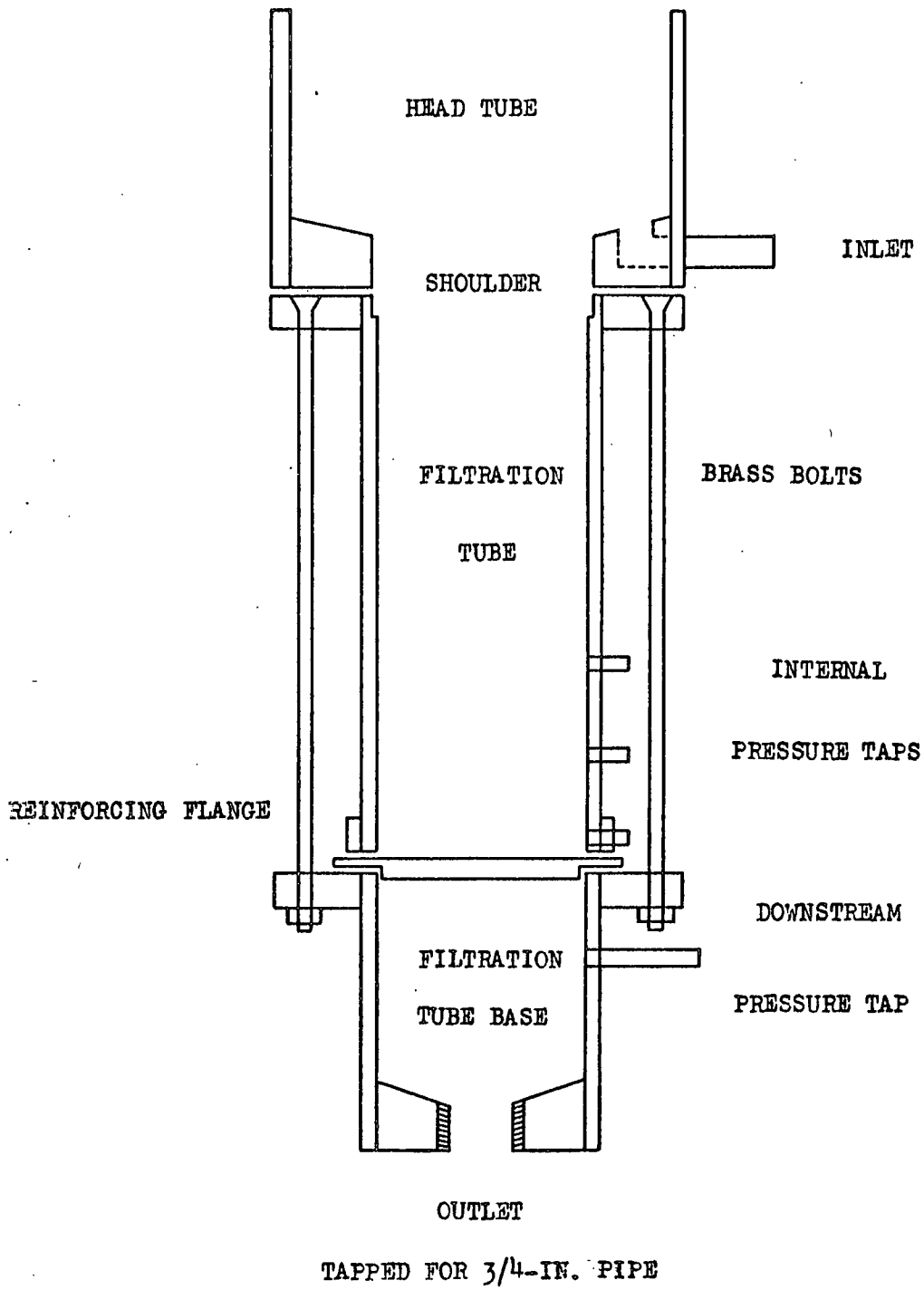

Figure 2 Filtration Tube Assembly

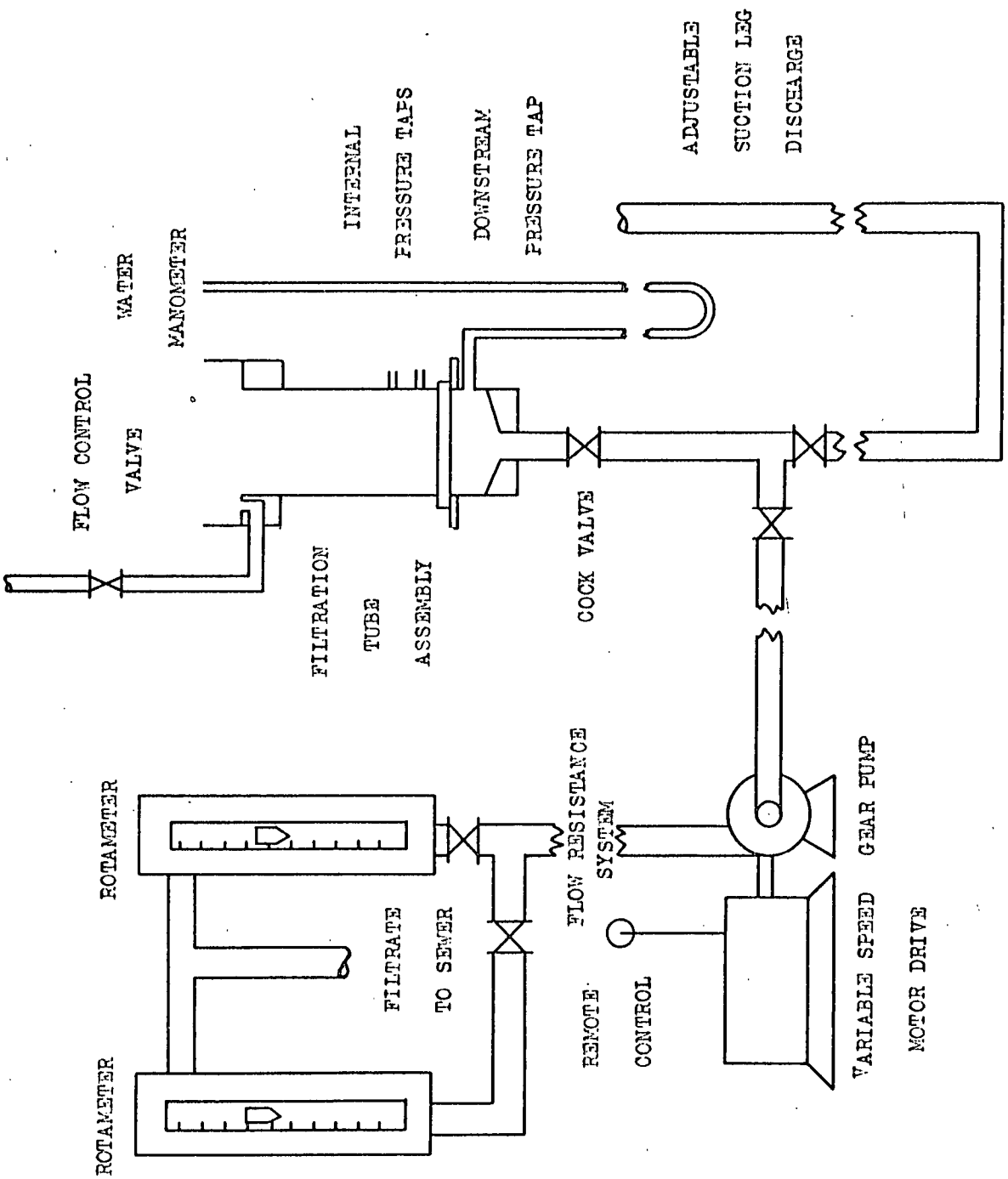

Figure 3 Filtration and Thickening Apparatus

one side of the bottom was countersunk a 3/8-in. hole, which connected at right angles with a Lucite tube penetrating the side wall of the head tube. This was the stock and water inlet, and served to maintain a smooth flow in the filtration tube proper. The bottom tapered 1/4 in. down from the side wall to the filtration-tube entrance to provide free drainage. The head tube was gasketed with a 1/16-in. rubber gasket and bolted to the filtration tube with four brass bolts.

The filtration tube sat on a brass septum. This septum was a 3-3/4-in. brass plate, shouldered to fit snugly on the Lucite filtration tube base. It was drilled with 3/16-in. holes on 1/4-in. closepacked centers. It was covered with 30-mesh screen, which in turn was covered with 150-mesh screen. The screens were soldered to the plate around the edge, with excess solder left on top. This excess was turned down to provide a smooth plane surface to make a seal with minimum pressure with the gasket on the bottom of the filtration tube.

The Lucite filtration-tube base, on which the septum and filtration tube sat, was a four-inch section of 3-1/8-in. I.D., 3-1/2-in. O.D. Lucite tubing. To it was glued a one-inch thick Lucite base, which was drilled and tapped for a 3/4-in. standard pipe. There was one 3/16-in. I.D., 5/16-in. O.D. pressure tap and water feed set into the side wall of the base tube. To the top of the tube was glued a six-inch flange of 1/2-in. Lucite. A 1/16-in. rubber gasket was glued to the top of the filtration tube and flange.

The filtration tube, septum, and base were assembled and clamped together with two long brass bolts. The heads of these bolts were sunk in

the flange glued to the top of the filtration tube. The bolts extended through the flange on the top of the filtration-tube base and were secured with washers and wing nuts.

Auxillary equipment designed and built by Ingmanson (5) was used in determining the compressibility of the pulp. This equipment consisted of a permeable piston mounted on a rod, a cover plate for the head tube, and cylindrical weights which could be placed on the rod. The permeable piston was a perforated brass plate similar to the septum, covered with 40- and 150-mesh wire screens. This fitted smoothly into the filtration tube and was provided with a three-inch-high brass sleeve, 1/64-in. thick. This sleeve fitted flush with the outer edge of the piston. This assured proper alignment of the piston in the tube. A 1/4-in. brass rod screwed into a stub on the inside of the piston and passed through a hole in the brass cover plate, which thus kept the rod centered in the tube. The weights slipped over the end of the rod and were retained by a shoulder, providing the desired compacting pressure when used.

A close-fitting, low-friction, impermeable piston was made to seal off the top of the pad during thickening runs. The piston was a hollow brass cup, 3-1/2-in. high, with 1/32-in. walls and a 3/32-in. base. The piston weighed 245 g. The piston was machined to a very close fit with the Lucite filtration tube at 25.4°C. The fit was very temperature sensitive because of the difference in the coefficients of thermal expansion of Lucite and brass.

The over-all layout is shown schematically in Figure 3. A 3/4-in. galvanized-iron pipe was fitted into the tapped hole in the base of the

filtration tube. This led to a brass plug cock, which was followed by a tee of the same diameter. One side of the tee led to a suction leg, the down side of which was galvanized iron, and the up side flexible rubber tubing. The other side of the tee was adapted for 1/2-in. copper tubing, and led to a constant-volume pump.

The pump was a Maisch gear pump driven by a continuously-adjustable variable-speed Graham drive, which was in turn driven by a synchronous motor. The volumetric discharge flow rate was rated at 0 to 150 cc./sec. The discharge side of the gear pump was equipped with a pressure gage and safety pop valve. Following in the discharge line was a needle throttling valve and a maze of four orifices. The throttling valve and four orifices were arranged in parallel with by-passes. The first orifice was 1/16-in. in diameter, and the other three were 1/32 in. in diameter. These flow-resistance devices were necessary to build up a back pressure of about 30 psi. on the pump in order to minimize drift and pulsation at the lower flow rates.

After the flow resistance system, the flow passed through one of two rotameters. One had a capacity range of 1 to 15 cc./sec. of water, and the other a range of 10 to 75 cc./sec. of water.

There were two pressure-recording systems available. The first was a Brown "Electronik" single-point recording potentiometer, model no. Y153X12(X)-X-9A1A3(D) with a full-scale response of under four seconds. This was used in conjunction with a Manning, Maxwell, and Moore electronic pressure transmitter, type 145, LV-1/4L, with a range of 0 to 40 in. of water vacuum. The volumetric displacement change of the pressure-sensing bellows was nearly five cc. over full-scale deflection of 100 cm. of water.

A two-meter water manometer was used as an indicating device with this system.

The second pressure-recording system was composed essentially of a series of manometers and a camera. There were ten 8-in. mercury-filled manometers of 3-mm. internal diameter. One side of each was water-connected through plastic tubing to a pressure tap in the filtration tube or base. The other side of each manometer was vented to the atmosphere through a glass-wool air filter. The ten manometers were all mounted on a single board, which provided for measuring all of the pressures in the system. The volumetric displacement for a pressure change of 100 cm. of water was only 0.54 cc. per manometer. This minimal displacement was necessary to avoid disruption of the pad by the introduction of excessive fluid into the pad through the side wall taps during the course of a run.

Mounted on the same board as the manometers was a scale-reading electric clock and two rulers divided into 0.02-inch divisions. The board itself was mounted on a steel and plywood frame, on which was also mounted a Voigtlander Vitessa camera to record the pressure as a function of time. This 35-mm. camera had a special rapid-winding feature which enabled a full roll of 36 exposures to be taken manually in less than 30 seconds. When used at 1/250 seconds with a Kodak Porta #2 lens attachment and Adox KB-14 ultra-fine-grain-film, this camera was capable of clearly resolving the scale divisions and "stopping" the 1/10-second dial on the clock.

Water or pulp slurry could be fed into the head tube or filtration-tube base by gravity flow from a 17 by 17 by 21-inch copper head tank elevated two feet above the top of the head tube. The flow rate was

adjusted by means of a screw clamp on a section of rubber tubing. The water was warmed and desupersaturated by injection of steam and air into the water supply line to the tank. Tap water and steam, both filtered through Fulflo 27R8 cotton filters, were mixed in a 1/2-inch Penberthy injector. Air, similarly filtered, was injected further down the pipe and the mixture sprayed into the head tank. This procedure warmed the water to the desired temperature and removed the supersaturating air. This produced a water free from suspended solids and air bubbles. Around the top of the tank was a wash pipe, a 1/2-inch copper pipe drilled with 1/32-inch holes on one-inch centers in such a way as to spray the inner walls of the tank with water. This was used in cleaning the tank. A rheostat-controlled Lightnin' mixer was mounted on the tank. An overflow and bottom drain were provided.

The filtration-tube assembly, rotameters, suction leg, and some auxillary equipment was mounted on a 1-1/2-inch-angle iron frame.

EXPERIMENTAL PROCEDURES

DETERMINATION OF SEPTUM RESISTANCE

In all of the mathematical expressions developed, it has been assumed that all of the resistance to flow is associated with the pad of pulp. However, there is some resistance associated with the septum. The pressure drop across the septum was determined at the maximum flow rates used in the experimental program. The filtration tube was filled with filtered, desupersaturated water and the water manometer read. The constant-rate pump was then started, and the manometer read at 45 cc./sec., which was in the maximum flow range used. At 21°C., the pressure drop was less than 0.25 cm. of water, a negligible effect. At this flow rate, the Reynolds number in the tube is only 810, which is well within the laminar range. As this is the most nearly turbulent flow encountered, all the flows in this work must be laminar.

DETERMINATION OF PISTON FRICTION AND LEAKAGE

Another source of pressure drop in the system was the frictional resistance of the piston sliding down inside the filtration tube. This friction was found to be a strong function of two factors, temperature and clamping of the tube. The temperature was a factor because the coefficient of thermal expansion of Lucite was 90×10^{-6} per °C., while that of brass is only 18.8×10^{-6} per °C. The clamping of the filtration tube to the base was a factor because of the flexibility of the Lucite. Even light clamping was sufficient to distort the tube appreciably from the true round, and thus to change the frictional resistance markedly.

To determine the pressure drop arising from the frictional resistance of the piston, the filtration tube was filled with water at a controlled temperature and a constant head maintained after the pump was turned on. The manometer was read, and the piston inserted into the tube, still maintaining the same constant head. The manometer was then read as the piston moved down the tube at a rate governed by the rate of water withdrawal maintained by the constant-rate pump. The manometer readings were then corrected for the net weight of the piston immersed in water, and the difference between the corrected reading and the initial reading without the piston was the frictional resistance of the piston. It was found that this resistance, in the range of flow rates of interest, was 1.5 ± 0.5 cm. of water pressure or $7.35 \pm 0.25 \times 10^4$ dynes. This was at 25.4°C. and employing minimal clamping of the tube. The variation, 0.5 cm. of water was felt to be negligible, and so a constant correction of 1.5 cm. was applied to all further data to compensate for piston friction.

The leakage of water past the piston under these conditions was also determined. The piston was supported at a point approximately one-half the distance up the tube, and the suction leg of the apparatus adjusted to create a known pressure drop across the piston. The flow was measured by timing the effluent into a graduate. The flow rates for various pressure drops are given in Table II.

TABLE II

PISTON LEAKAGE vs. APPLIED PRESSURE DROP

$P/\rho g.$, cm. H_2O	q, cc./sec.
30	0.06
58	0.14
94	0.20

This leakage is negligible, considering the flow rates actually used, (4 to 8 cc./sec.), and may be neglected.

PULP PREPARATION

The pulp used, a western full-bleached sulfite, was obtained in the form of airdry laps. The laps were torn up and soaked for 24 hours at 3% consistency. The pulp was then defibrated for 10 minutes in the Williams disintegrator. After dewatering in a large Buchner funnel, the pad was broken up and passed through a laboratory shredder. The shredded pulp was thoroughly mixed and stored at 34.3% ovendry consistency in plastic bags in a dark room maintained at 8°C.

Before using any pulp, the required amount was weighed out and soaked overnight at room temperature at 1% consistency. It was then disintegrated at 0.5% consistency for 23 minutes in a standard British disintegrator. The slurry was then transferred to a four-liter suction flask and deaerated with a water aspirator. The deaeration was essentially complete after thirty minutes.

DETERMINATION OF FILTRATION RESISTANCE AND COMPRESSIBILITY

The average specific filtration resistance of the pulp was determined using the method described and used by Ingmanson and Whitney (8). The static compressibility of the pulp was determined by the method of the same authors.

The pulp was dispersed at approximately 0.01% consistency in the head tank. The filtration tube was then filled with slurry to the zero mark.

The constant-rate pump was then started coincidentally with the Brown - Microsen pressure-measuring system. During the run the flow and head were held constant. When the pressure reached the limiting value of the recording system, the pump, cock valve, feed to head tube, and recording system were shut off. The water temperature, head height, and flow rate were recorded. The remaining slurry in the tube was filtered by draining through the pad. From these data and the ovendry weight of the pad the average specific resistance of the pulp on a mass basis may be calculated as a function of the frictional pressure drop across the pad.

The pad was then allowed to expand for ten minutes, at the end of which the permeable piston was introduced into the tube. This piston was then loaded with the weights, and the pad height measured with a cathetometer as a function of the loading pressure, allowing one to three minutes for equilibration after loading. The endpoint at which equilibrium was assumed was somewhat arbitrary in nature. It was that point at which the frictional pressure drop across the pad was not detectable on a water manometer. There was only a very slight change after this point. The pad was then removed, dried overnight at 102°C., and weighed. From these data the pad concentration may be calculated as a function of applied load.

THICKENING STUDIES

During thickening runs with the apparatus constructed for this work, it was found that a standardized procedure was essential to the reproducibility of the data. The following procedure was developed and adhered to.

Shortly before use, the feed tank was filled with filtered, desupersaturated water. The Microsen pressure transmitter and the Brown recording

potentiometer were allowed at least a 15-minute warm-up. Water was then introduced from the feed tank into the filtration tube through the tap beneath the septum until the water level was up to the zero mark on the tube. The water was shut off, and the manometer and recorder zeros were read. The variable-speed gear pump was then started and the pump speed and throttling system were adjusted to give the desired flow rate with about 30 p.s.i. back pressure on the pump.

The water level was allowed to drop to about one inch above the septum and the previously prepared pulp slurry (at 0.5 to 1.0% consistency) poured in, continuing the pumping. The slurry level in the tube was maintained by the addition of any remaining slurry. When all the slurry was in the tube, the pump was stopped and the cock valve at the bottom of the tube shut. A small motor-driven stirrer was then used to redisperse the pad. The stirrer was then removed and the constant-rate drainage again started.

The level was allowed to drop just to the bottom of the head tube, and all fibers hanging up in the head tube were washed down into the filtration tube. The level was then again brought up to the zero mark with water from the feed tank introduced through the side inlet in the head tube. The level was maintained thereafter by a suction overflow. During this pad formation, some agitation was essential, due to the high consistency used (0.5 to 1.0%). A stirring rod was used to provide this agitation, which was found to be quite critical. However, after some practice, reproducible pads could be formed, in which the affects of flocculation and creep were minimized, and tended to cancel one another out. This was an attempt to form pads which gave frictional pressure

drops in the permeation which agreed with the frictional pressure drops calculated from the filtration-resistance data.

Water, at 25.1 to 25.8°C., was kept permeating through the pad just until the system approached equilibrium, with respect to temperature, pressure drop, and pad volume. This required only one to three minutes. The cathetometer was then focused at a given height above the septum. This height was such that it would mark the original position of the top pad face, as calculated from Equation (31) using the values of $\underline{c}$ and $\underline{R}$ as functions of pressure, and the pad weight, flow rate, and temperature.

The impermeable piston was then submerged in the head tube and guided into the filtration tube proper. At the instant the piston reached the cross hairs in the cathetometer, the Brown-Microsen pressure-recording system was started. At the same moment, the scale-reading electric timer on the manometer panel could be started and during the thickening pictures taken of the manometers and clock, if the pressure distribution within the pad was desired. When the pressure reached the limit of the pressure-recording system, the pump was shut off, the plug cock closed, and the manometer-board clock and the Brown-Microsen system stopped. The final position of the piston was measured with the cathetometer.

To run duplicates, the pad and piston were lifted to the head tube by the introduction of water from the feed tank at the tap beneath the septum. The piston was removed, and the pad redispersed and reformed. In view of the fact that the pulp was unbeaten, it was not unexpected to find that the pad could be reused without any significant variation in results. The pad was then oven dried overnight and weighed.

The film, Adox KB-14, was developed in Kodak Finex developer. It was then projected on a smooth screen and the mercury differentials measured with a ruler. The timer in each frame was read to the nearest 0.1 sec.

EXPERIMENTAL RESULTS AND DISCUSSION

ORIGINAL DATA

The original data obtained in the course of this work are not presented in this thesis. They were recorded in three different manners, and much is not amenable to direct presentation. Each run was numbered, and where data were recorded in more than one form, the run number serves as the cross reference. These data are available at the Institute of Paper Chemistry.

The basic data about each run were recorded in Institute Research Notebook no. 1360. These data included cathetometer, thermometer, rotameter, and chart speed readings, where needed. Also included were zero settings and all other pertinent auxilliary data. The Brown-Microsen pressure-recording system was used for over-all pressure-drop recordings, and the data were obtained as continuous curves on strip charts, which were labeled with the run numbers. The internal pressure distribution data were obtained in the form of 35-mm. negatives, with the run number visible in each run.

CALCULATION DATA

The data needed for the calculation of the path of a thickening are the point specific filtration resistance of the pulp and the point compressibility of the pulp, both as functions of mechanical compacting force. What was actually determined was the average specific filtration resistance and point pad concentration as a function of compacting load. In Table III are presented the summarized average-specific-resistance data and their deviations from the means, as determined by constant-rate filtrations in

triplicate. In Table IV are presented the pad-concentration data as a function of applied load as determined by static-loading experiments in quadruplicate. The precision of this data is noted and is well within the limits needed for this work.

From this data can be calculated first the point specific resistance on a mass basis ($\underline{R}$) and point compressibility on a mass basis ($\underline{Y}$) as functions of the mechanical compacting stress, and then from this the course of any thickening of this pulp. Only a brief indication of the method will be given in this place, but a more complete discussion will be found in Appendix II.

The point specific resistance is determined by a visual graphical differentiation and algebraic manipulation of a plot of the average specific resistance *versus* over-all frictional pressure drop. The point compressibility is determined by a visual graphical differentiation of a plot of reciprocal pad concentration *versus* compressive stress, which has been extrapolated to effectively zero stress. It is interesting to note that this data indicates the concentration at the pad face during a filtration under these conditions to be only about 1% by weight. Thus, the pad must have an appreciable mechanical strength even at this low concentration.

The conversion to tau units is now made. The reciprocal point specific resistance is plotted *versus* compressive stress, and graphically integrated along the range to evaluate τ and $\underline{k}$ from Equations (20) and (21). In order to establish the average pad volume per gram of pad solids for pads of this pulp under permeation, the reciprocal point concentration ($1/\underline{c}$) is plotted against a measure of mass fraction $\underline{M}'$, and integrated across the pad for the various pressure drops under consideration.

TABLE III

AVERAGE SPECIFIC RESISTANCE

Western Bleached Sulfite

$\Delta P_f/\rho g.$, cm. H_2O	$\bar{R}_{av}$ x10^{-8} Mean	Av. Deviation from Mean, %
1	0.149	4.7
3	0.263	2.9
6	0.341	0.4
11	0.438	0.8
21	0.596	0.8
31	0.729	0.8
41	0.845	0.9
51	0.951	1.1
61	1.051	1.0
71	1.146	1.2
81	1.240	1.1
91	1.334	0.7

TABLE IV

PAD CONCENTRATION VS. LOADING

Western Bleached Sulfite

Load $P/\rho g.$, cm. H_2O	Pad Conc. g./cc.	Av. Deviation from Mean, %
9.55	0.0714	4.6
17.30	0.0864	2.2
26.30	0.1049	0.9
40.10	0.1256	0.6
63.20	0.1506	1.6
100.00	0.1775	2.1

The term BYR in Equation (34) may now be evaluated and plotted as a function of tau from Equation (33), the previously established relationships of $\underline{Y}$, $\underline{R}$, $\underline{P}_s$, and τ, and the particular conditions of the thickening under consideration.

The thickening itself is calculated using an iterative numerical method of solution of Equation (34). That is, the differential Equation (34) is approximated by a finite difference equation. The pad is considered divided into a finite number of discrete mass increments, and it is assumed that it is feasible to assign average values to the variables in each increment. The form of the results is that of a tau distribution on a mass fraction basis throughout the pad as a function of the volume fraction of the pad removed. That is, tau is obtained as a function of $\underline{M}'$ and $(1-\underline{v})$. This may be converted to give over-all pressure drop and internal pressure distribution on a volume-fraction basis as a function of time from start of thickening. In other words, tau or pressure may be obtained as a function of $\underline{M}'$ or $\underline{V}'$ and $(1-\underline{v})$ or θ.

OVER-ALL PRESSURE DROP THICKENING STUDIES

The basic plan of attack in these studies was to predict the over-all pressure drop across the pad as a function of time in a given thickening and then to experimentally determine the function. However, the theory proposed predicts, that if over-all pressure drops are plotted against the pad volume fraction removed, $(1-\underline{v})$, instead of time, all constant-rate thickenings starting from permeations at the same original pressure drop should fall on the same line. Here are, then, two tests of the theory. The first is whether plotting net over-all pressure drop ($\Delta\underline{P}$) against

(1-v) will reduce a family of thickenings of this type to a single line. The second test is how closely this line, if found, agrees with the theoretically predicted line.

In Figure 4 are plotted three average thickening curves as net over-all pressure drop versus actual time in seconds from the start of thickening. These three sets of runs all had the same expected initial over-all pressure drop, 29.5 cm. water, and were run at the same temperature. In Table V the pertinent facts about these runs are summarized, and in Figure 5 the runs in set A are plotted individually.

TABLE V

FLOW CONDITIONS FOR THICKENING RUNS

Set	No. Runs in set	Pad Wgt., grams	Flow Rate, cc./sec.
A	5	14.1	8.40
B	3	18.8	6.25
C	3	25.1	4.70

These curves illustrate the variation (Figure 5) and actual spread (Figure 4) in runs which are to be made to coincide by the transformation to a plot of pressure against (1-v) if the theory is correct. It will be noticed on these runs that the tests did not actually all start out exactly at the theoretical pressure drop of 29.5 cm. of water, as predicted by the measured filtration resistance of the pulp and Equation (2). This was because of deviations of the pad formation from the ideal, as will be discussed later.

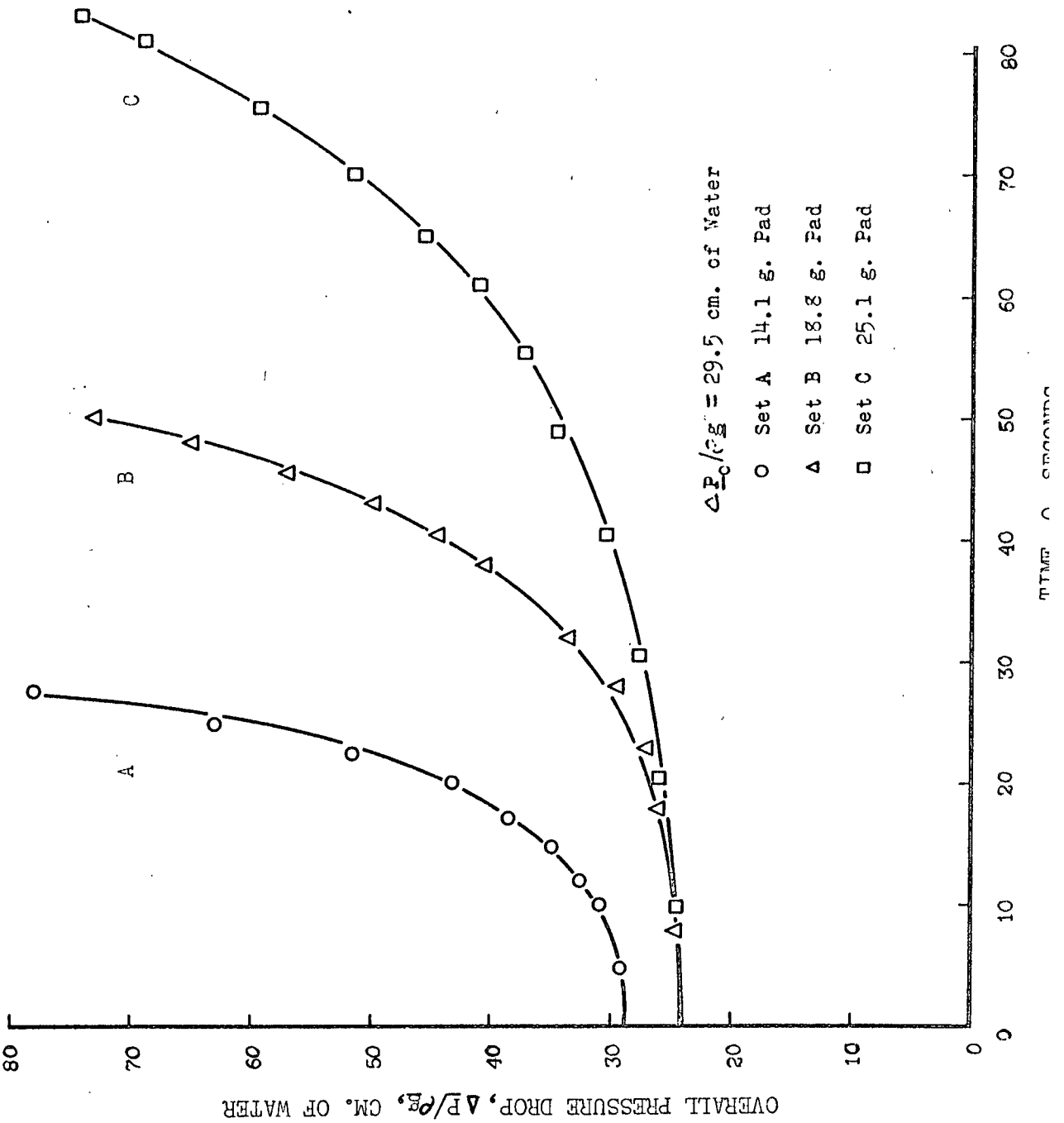

Figure 4 Observed Thickening Runs, Overall Pressure Drop versus Time

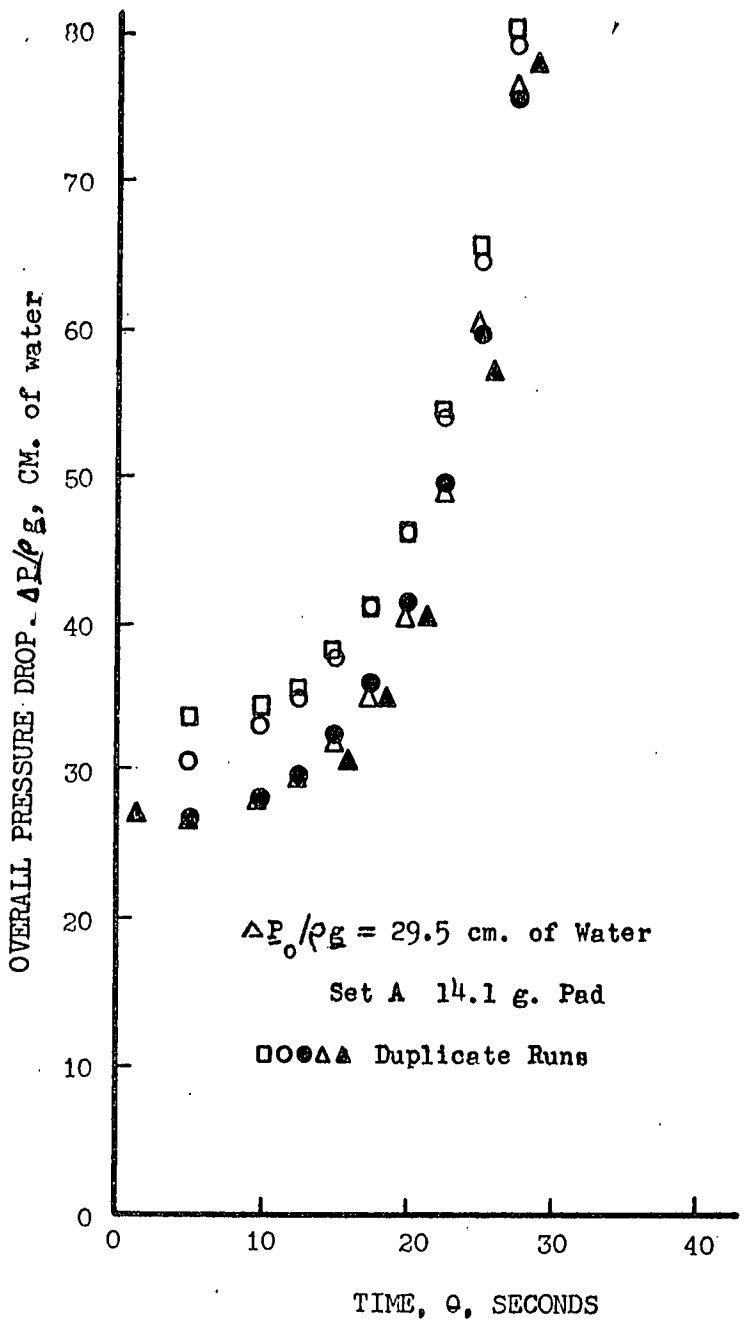

Figure 5 Individual Observed Thickening Runs, Overall Pressure Drop versus Time

In Figure 6 these same sets of runs from Figure 4 are replotted as net over-all pressure drop against (1-v), the volume fraction of the original pad removed, instead of time in seconds. It can be seen that these three curves now very nearly coincide, within the limits of experimental error, both in shape and in absolute magnitude. This is in agreement with the proposed theory.

In Figure 7 the arithmetic average of all the curves plotted in Figure 6 is plotted as over-all pressure drop versus (1-v). Also plotted is the theoretical curve predicted on the basis of the proposed theory. This curve was calculated as shown in Appendix II using only the derived mathematical expression of the postulated phenomenon and the filtration resistance and compressibility of the pulp as determined by independent measurements. The predicted curve is thus entirely independent of the observed results, and is actually a predicted curve, not a fitted curve. While the two curves, observed and predicted, do not coincide exactly, they agree within a few per cent, which is well within the expected limits of experimental error, as will be discussed later.

Two more sets of data of over-all pressure drop versus volume fraction removed are shown in Figure 8. This data is of the same type as that presented in Figures 5-7. For each set of runs at the same expected initial over-all pressure drop, 16.1 and 48.3 cm. of water, respectively, for the sets D and E, there is shown the predicted course as a solid line. The points are the experimentally determined values, the averages of a number of duplicate runs. Each symbol is for a set at a different pad weight and flow rate.

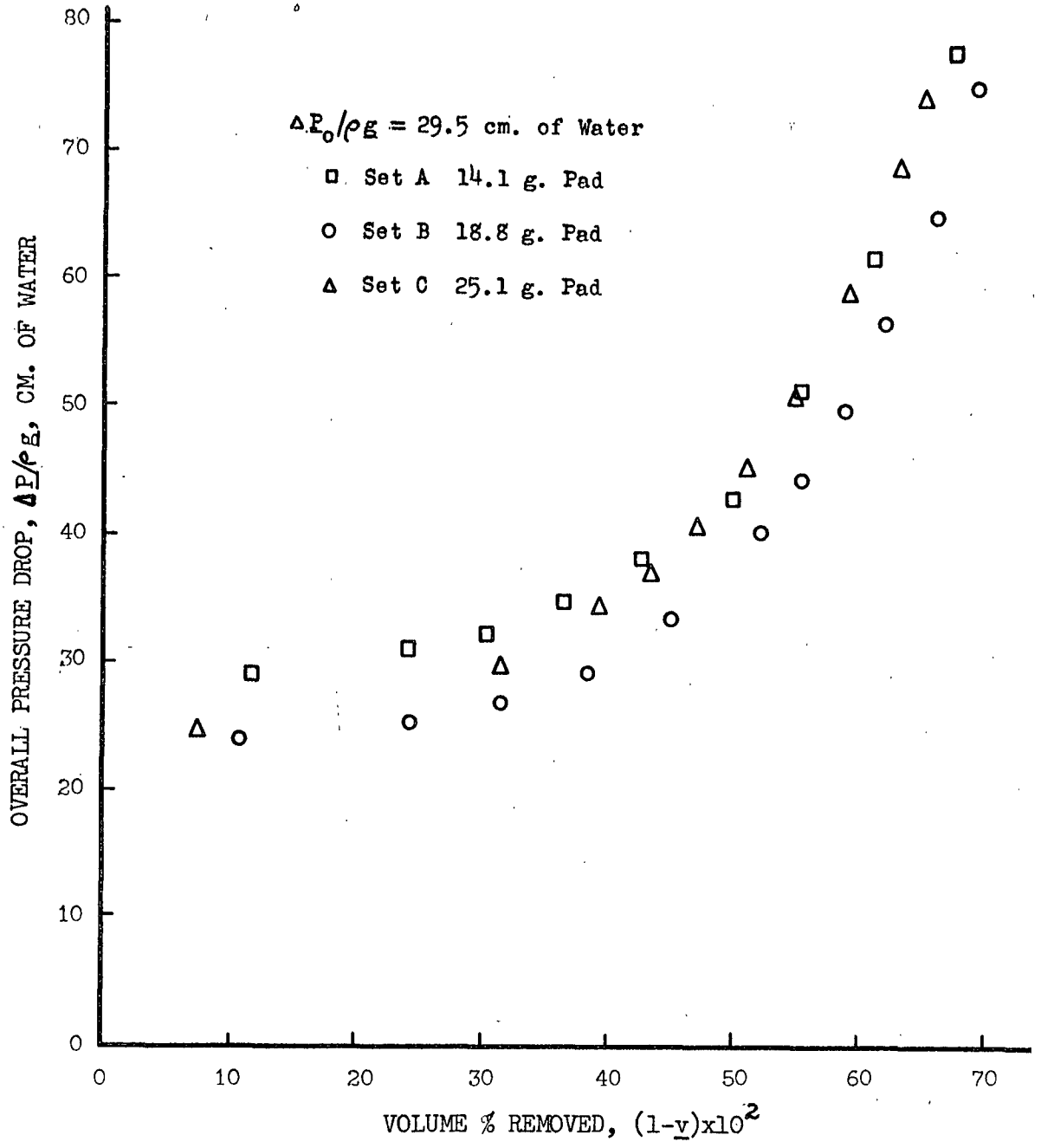

Figure 6 Observed Thickening Runs, Overall Pressure Drop versus Volume % Removed

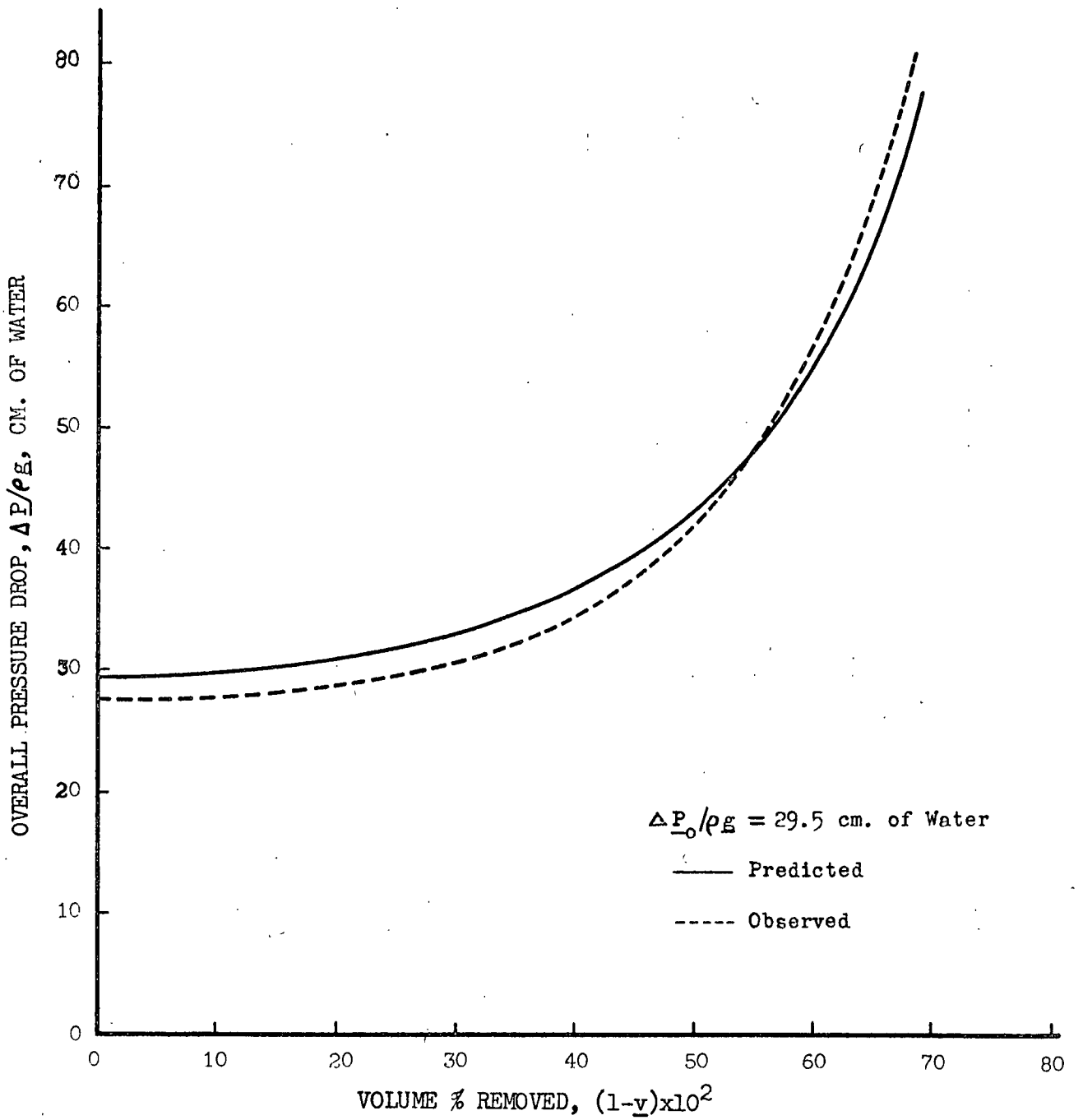

Figure 7 Observed and Predicted Thickening Runs, Overall Pressure Drop versus Volume % Removed

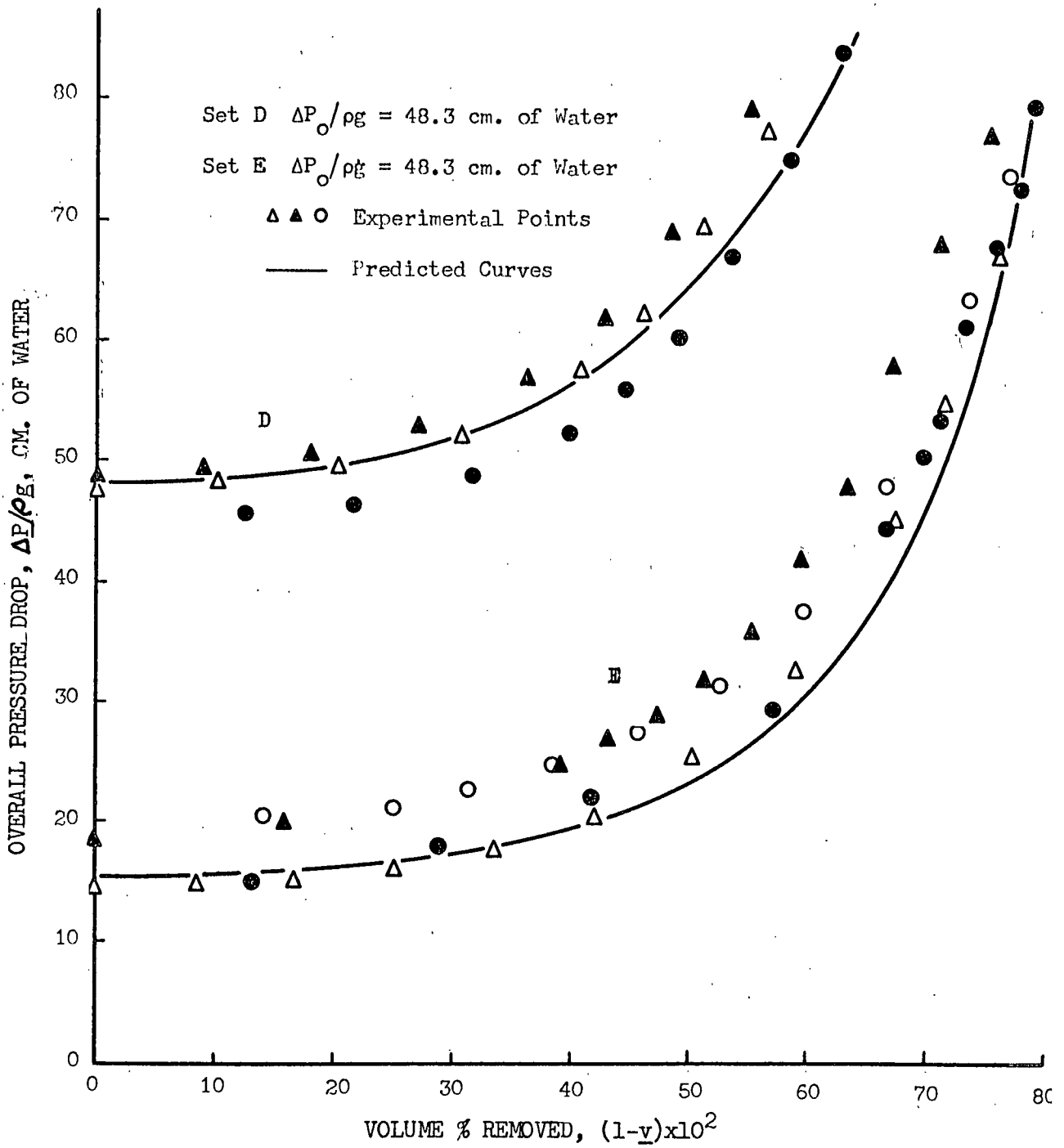

Figure 8 Observed and Predicted Thickening Runs, Overall Pressure Drop versus Volume % Removed

It will be noted that these two additional sets of data follow the same pattern as the first set presented in Figures 5-7. This is true with respect to the coinciding of the experimental curves when plotted on the reduced time basis, $(1-\underline{v})$, and the agreement between the predicted and observed curves. Thus, it is seen that the two tests of the proposed mechanism are satisfied by all of these sets of data.

Error Considerations

Upon critically examining these sets of data, comprising about thirty individual runs, a pattern may be noticed in the deviations of the experimental results from the predicted curves. The error, apparently, may be divided into two sections. The first type of error is in the original starting over-all pressure drop, which may deviate from the theoretical value by as much as 20%, in the extreme. Secondly, it is apparent that all the runs in one set, regardless of the individual starting pressures, tend, during the course of the thickening, to approach a line which does not exactly coincide with the predicted line, but which rather may be displaced a maximum of about 7% on the reduced time scale.

The causes of the first type of error are twofold. The two causes are flocculation during pad formation and creep of the formed pad. It will be recalled from Equation (8) that the theoretical initial pressure drop is calculated from permeation theory, utilizing the specific filtration resistance as determined from constant-rate filtration experiments at 0.01% consistency. The pad formed for thickening, however, was formed from high-consistency (0.5-1.0%) slurries and was undergoing permeation when the initial pressure drop was recorded.

The effect of the high-consistency formation technique was to promote flocculation and thus lower the actual specific resistance of the bed. Ingmanson and Whitney (8) have shown on the same type of pulp that increasing the slurry consistency from 0.01% to 0.60% decreased the specific filtration resistance about 10% while increasing to 1.0% decreased the resistance about 25%. These figures tend to be maximal, since no turbulence was maintained in the slurry to minimize or counteract the tendency toward flocculation. From this flocculation effect alone then, the initial observed over-all pressure drop might have been 25% lower than predicted.

The effect of permitting the pad to undergo permeation before the thickening was to permit the pad to creep. During a constant-rate filtration (such as was used in determining the specific resistance) each element of the pad is subject to a steadily and quite rapidly increasing load. During a permeation or constant-pressure filtration, however, the load on each element is either constant or only slowly increasing. This apparently permits the pad to creep and compact to a greater extent, which increases the specific resistance of the pad for the same applied load or over-all pressure drop. Ingmanson and Whitney (8) have shown that the filtration resistance of a pulp as determined by constant-pressure filtration may be as much as 20% higher than as determined by constant-rate filtration, and attribute the difference to pad creep. From this creep effect alone, then, the initial observed over-all pressure drop might be raised more than 20% over the predicted value.

Thus, it may be seen that from these two sources there may be an error of about $\pm$20% in the initial observed over-all pressure drop, depending upon

exactly how the pad is formed. This first type of error was minimized by standardization of the pad-formation procedure, but was never entirely eliminated.

The second type of error, which caused the calculated results to tend to deviate from the observed results as the thickening proceeded, seemed to arise from any or all of five causes. These five were:

1. A discrepancy between the measured and effective point specific filtration resistances during the course of the thickening.

2. A discrepancy between the measured and effective pad concentrations as a function of compacting load.

3. A bias introduced by the iterative method employed for obtaining solutions to the final equation.

4. Miscellaneous experimental errors.

5. Turbulence in the pad.

A discrepancy between the measured (by constant-rate filtration) and effective specific filtration resistances during the course of a thickening run could have arisen as discussed in connection with the error in the initial over-all pressure drop. That is, the pad might be more flocculated and nonuniform or more dense, from creep, in the thickening than in the filtration used to calculate the resistance. The effect that a 10% increase or a 15% decrease in specific resistance would have on the calculated course of a thickening is indicated in Figure 9. However, it should be noted that these figures are very generous, as flocculation and creep are minimized by the pad-formation techniques employed. Here, and in the following discussion, it is assumed that $\underline{c}$ and $\underline{R}$ are independent

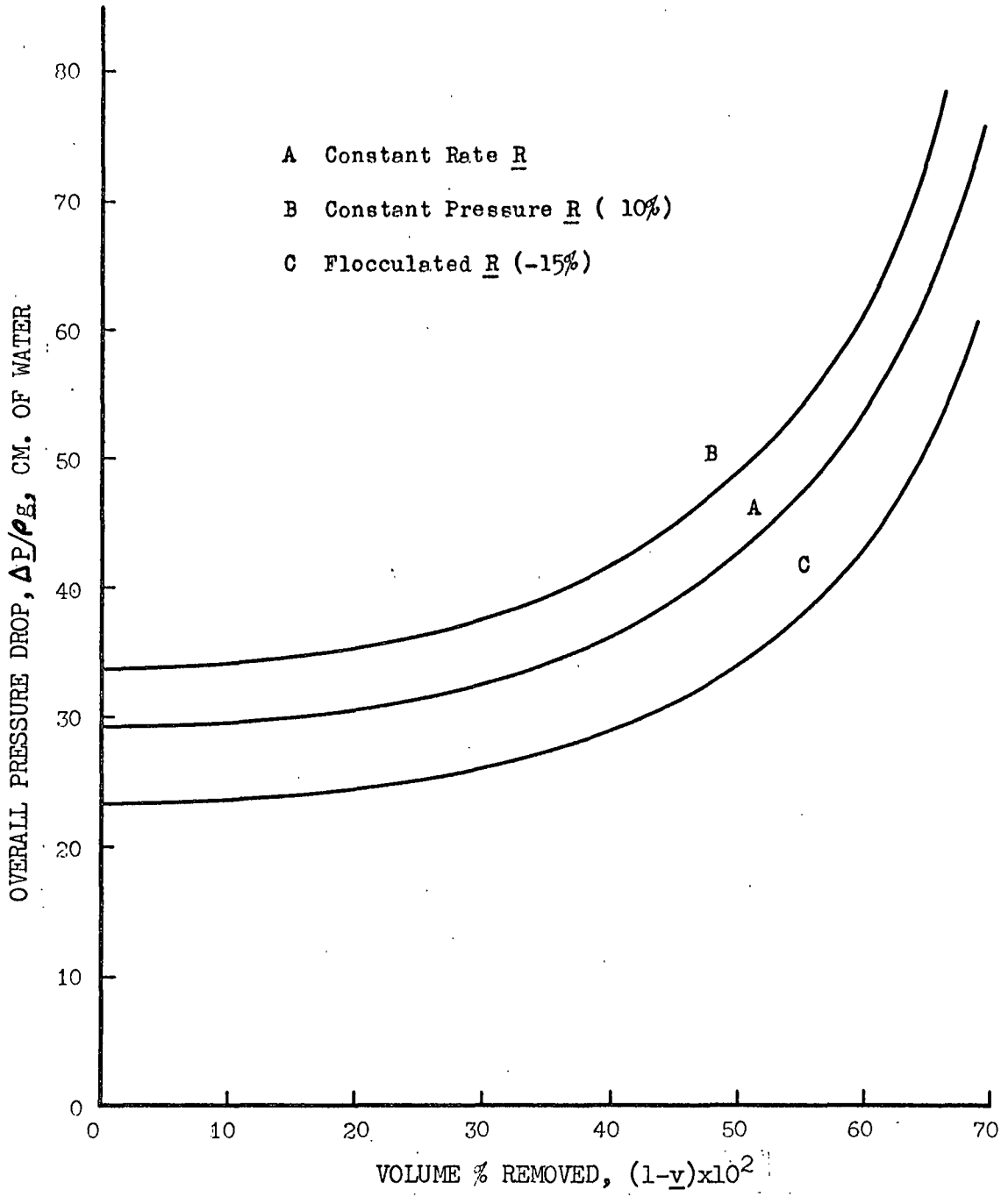

Figure 9 Effect of Variations in Resistance on Predicted Thickening Curves, Overall Pressure Drop versus Volume % Removed

functions of the compacting force. This is not actually true, but is a valid assumption in determining the separate effects on the calculated results as the two are measured entirely independently.

There might exist a discrepancy between the measured compressibility of the pulp and the effective compressibility during thickening, since creep plays a greater role in the static compressibility determinations than it does in the actual thickenings. This error would become important in the later stages of the thickening when the pressure is increasing quite rapidly. An indication of the difference in compressibility with and without this short time creep effect may be obtained from the data of Ingmanson and Whitney (15). From their data it may be seen that approximately a 15% higher pressure drop is required to compact a pad to a given average specific filtration resistance in a constant-rate filtration than in a constant-pressure filtration. In Figure 10 is given an indication of the effect of an increase of 15% in the pressure necessary to reach a given point consistency on the course of a thickening run. This effect is seen to be of minor significance.

The third source of error is in the actual iterative solution of the final partial-differential equation. This type of solution is by its very nature approximate only. By this method of solution two types of error may be introduced,--oscillation and bias. It was found possible to eliminate oscillation to an acceptable degree. Bias, however, is not as easily detected or eliminated. However, bias in any solution may be estimated by repeating the iterative solution utilizing finer subdivisions, in both pad thickness and time. However, these two must be reduced in such a way as to maintain $(\Delta \underline{m})^2/\Delta\theta$ or $(\Delta \underline{M'})^2/\Delta(1-\underline{v})$ approximately constant at equivalent points in the solutions.

Figure 10 Effect of Variation in Compressibility on Predicted Thickening Curves, Overall Pressure Drop versus Volume % Removed

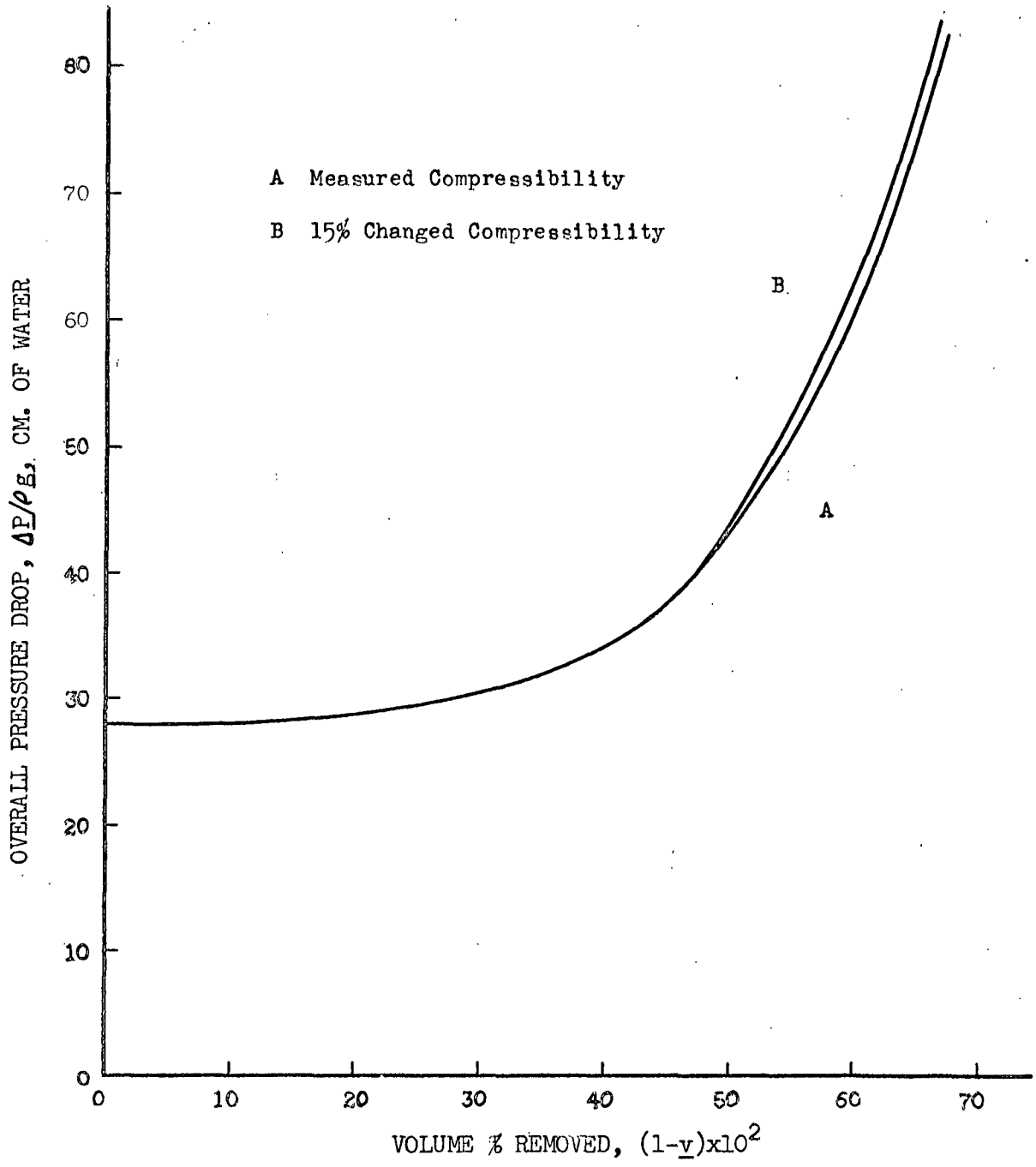

In Figure 11 are plotted two iterative solutions for the same thickening run. The only difference lies in the number of subdivisions employed in the solution. Curve B was calculated using approximately 2.4 times as many subdivisions as were used for curve A. This indicates that the error in curve B should only be about 40% of the error in curve A. Therefore, the difference between the two curves should be about 60% of the error in curve A or 150% of the error in curve B. But the maximum difference between these curves is only 5%, so the error in curve B should be about 3.5% and the error in curve A about 8.5%. The conclusion was thus reached that the calculated curves are in error (due to the calculation method) less than 10% at the end of a run, and considerably less at all earlier points. This accuracy is acceptable in this work. It is to be noted that the true solution apparently lies above the calculated curves in this plot. That is, it would give higher pressures at the same time intervals. This would tend to move the theoretical curve nearer to the observed results.

The fourth class of error in the observed results is that arising from purely mechanical causes. While these errors were minimized as much as was considered feasible, they were not eliminated. These errors arose from such things as time lags in the pressure-measuring system, leakage past the piston, and flow into the pad from the manometer bank. The composite effect was no more than a few per cent, which was not an important effect in this work.

The fifth possible source of error is the chance for turbulent flow inside the pad. Carman (16) had defined a modified Reynolds number for

Figure 11 Effect of Variation in Number of Subdivisions on Predicted Thickening Curves, Overall Pressure Drop *versus* Volume % Removed

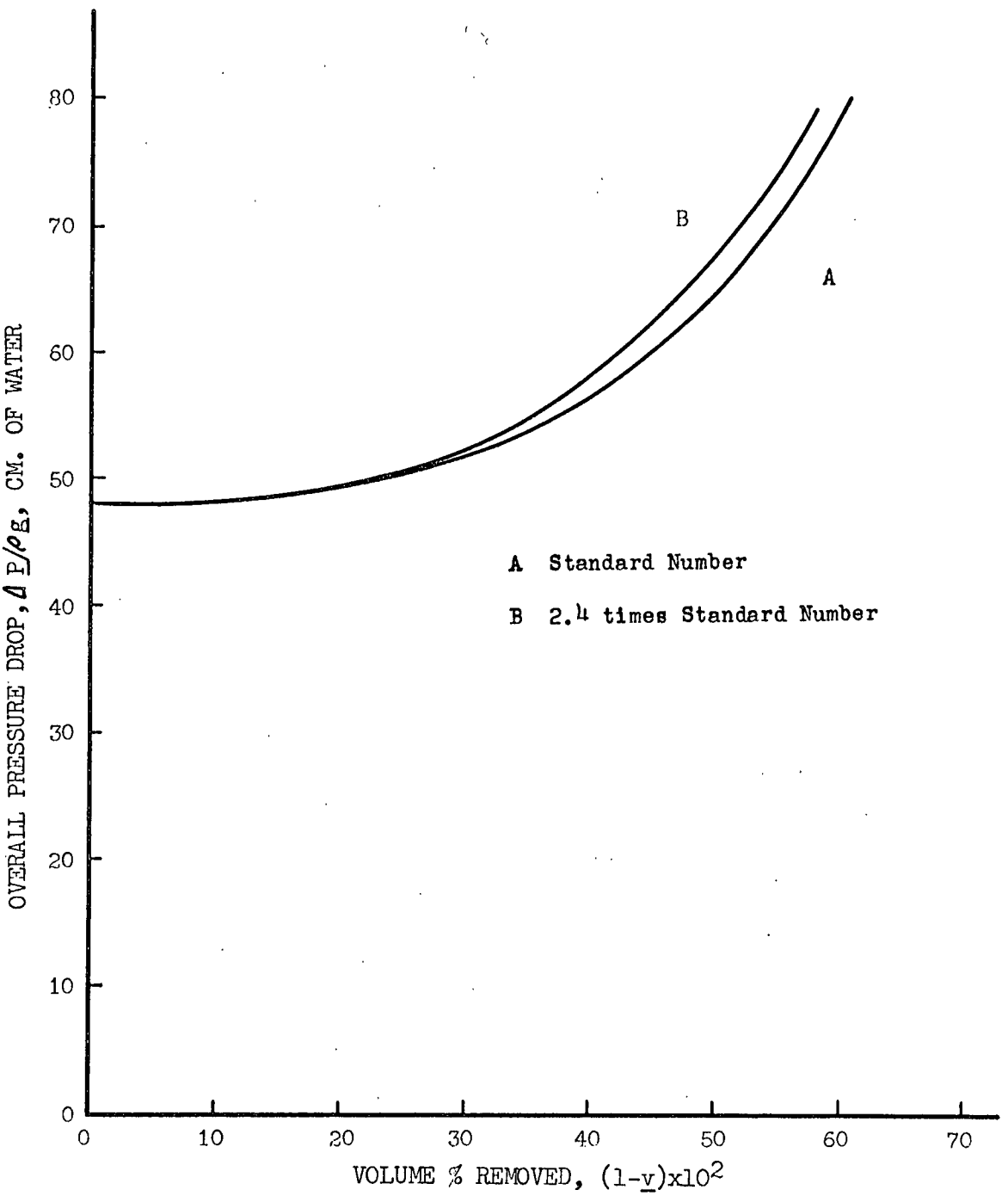

flow through porous beds. At no point in the work did this number exceed one-tenth of the critical value for the onset of turbulent flow. Thus, the requirement of laminar flow for the theoretical development was satisfied in the experimental work.

INTERNAL PRESSURE DISTRIBUTION STUDIES

The internal pressure distributions in a pad undergoing thickening were determined experimentally and compared with those predicted by the proposed theory. In the section on the postulated mechanism of thickening, it was shown that the solution of the final equation in terms of $\underline{P}_s$, $\underline{M}'$, and $(1-\underline{v})$ was dependent only on the material and the original pressure drop across the pad, in the case of thickenings which are constant-rate continuations of permeations.

It was found convenient to express the internal pressures as functions of the instantaneous pad-volume fraction $\underline{V}'$ instead of the analogous mass fraction $\underline{M}'$. This instantaneous pad volume fraction $\underline{V}'$, or per cent $\underline{V}' \times 10^2$, is a means of indicating a specific internal plane in the thickening pad. That is, a position in the pad indicated as $\underline{V}'=0.20$ would have 20% of the total pad volume, at that time, above it, and 80% of the total pad volume would be between that point and the septum. Once again, as in the over-all pressure drop studies, there are two checks on the validity of the theory. The first check is whether the internal pressure distribution ($\underline{P}_s$ as a function of $\underline{V}'$) at any given over-all pressure drop is a function only of the original over-all fractional pressure drop across the pad at the onset of thickening. That is, in a series of constant-rate thickening

runs of different pad weights and flow rates, but starting at the same initial over-all pressure drop, the internal pressure distributions at a given over-all pressure drop should be identical. The second check is how well these experimentally determined internal pressure distributions agree in magnitude and shape with the predicted curves.

In Figure 12 are plotted experimental internal-pressure-distribution data points from separate sets of thickenings. These sets all started from the same original expected pressure drop, but the pads were of different weights, and the flow rates were different. Three over-all pressure drops during the course of the run were chosen arbitrarily, -- 30, 50, and 70 cm. of water. The internal pressure distribution measured in each run is plotted. It will be noticed that the agreement between the points is quite good, well within the limits of possible experimental error.

The predicted internal pressure distribution is also indicated at each over-all pressure drop in Figure 12; it is shown by a solid line. It will be noticed that the agreement between the theoretical and experimental internal pressure distributions is as good as that between the sets of experimental data.

In Figures 13 and 14 are presented data similar to that in Figure 12, but for runs started at different over-all pressure drops. The agreement in Figures 13 and 14 is not noticeably different from that in Figure 12. The close agreement within the reduced experimentally determined pressure distributions and between them and the theoretically predicted pressure distributions is a confirmation of the validity of the proposed theory and mechanism.

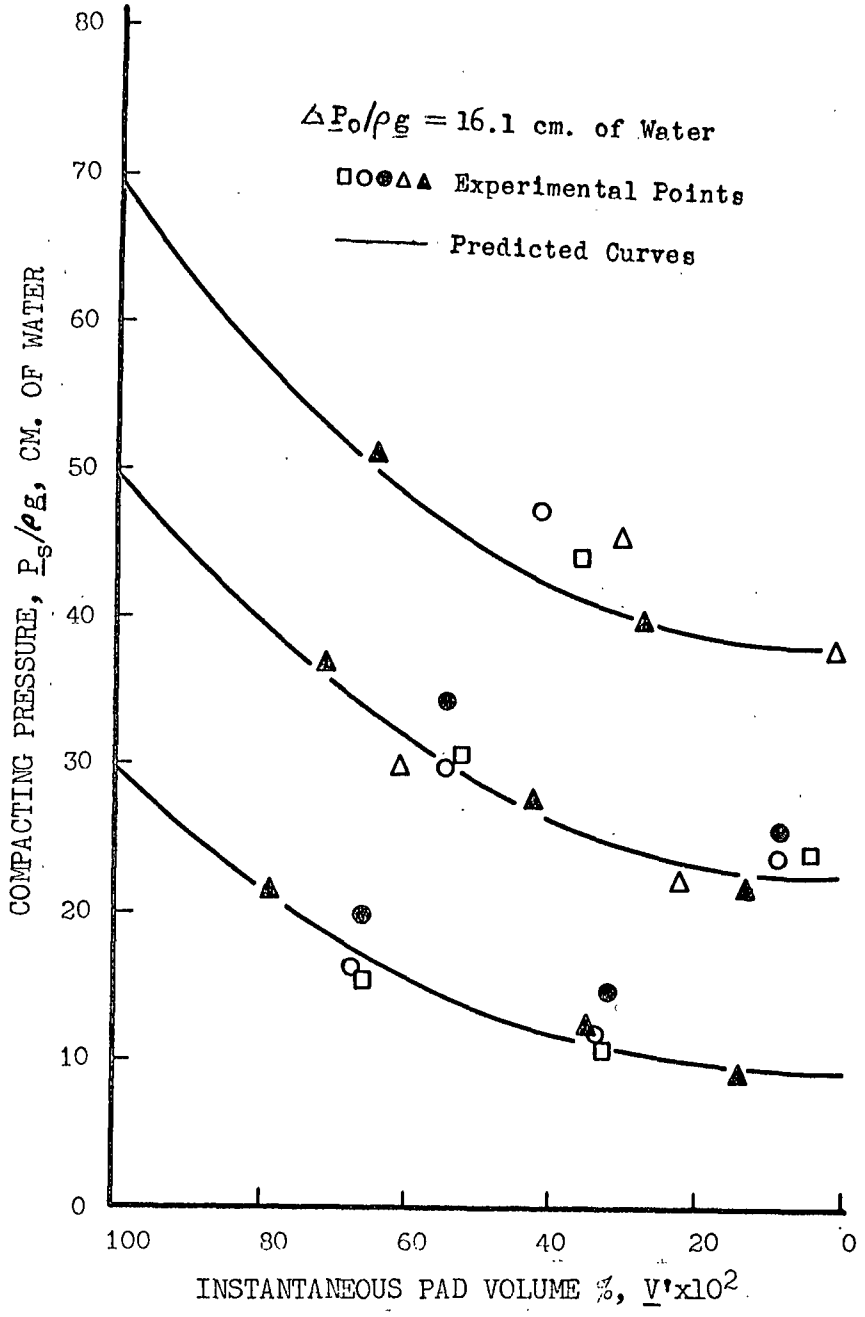

Figure 12 Internal Pressure Distributions, Compacting Pressure versus Instantaneous Pad Volume %

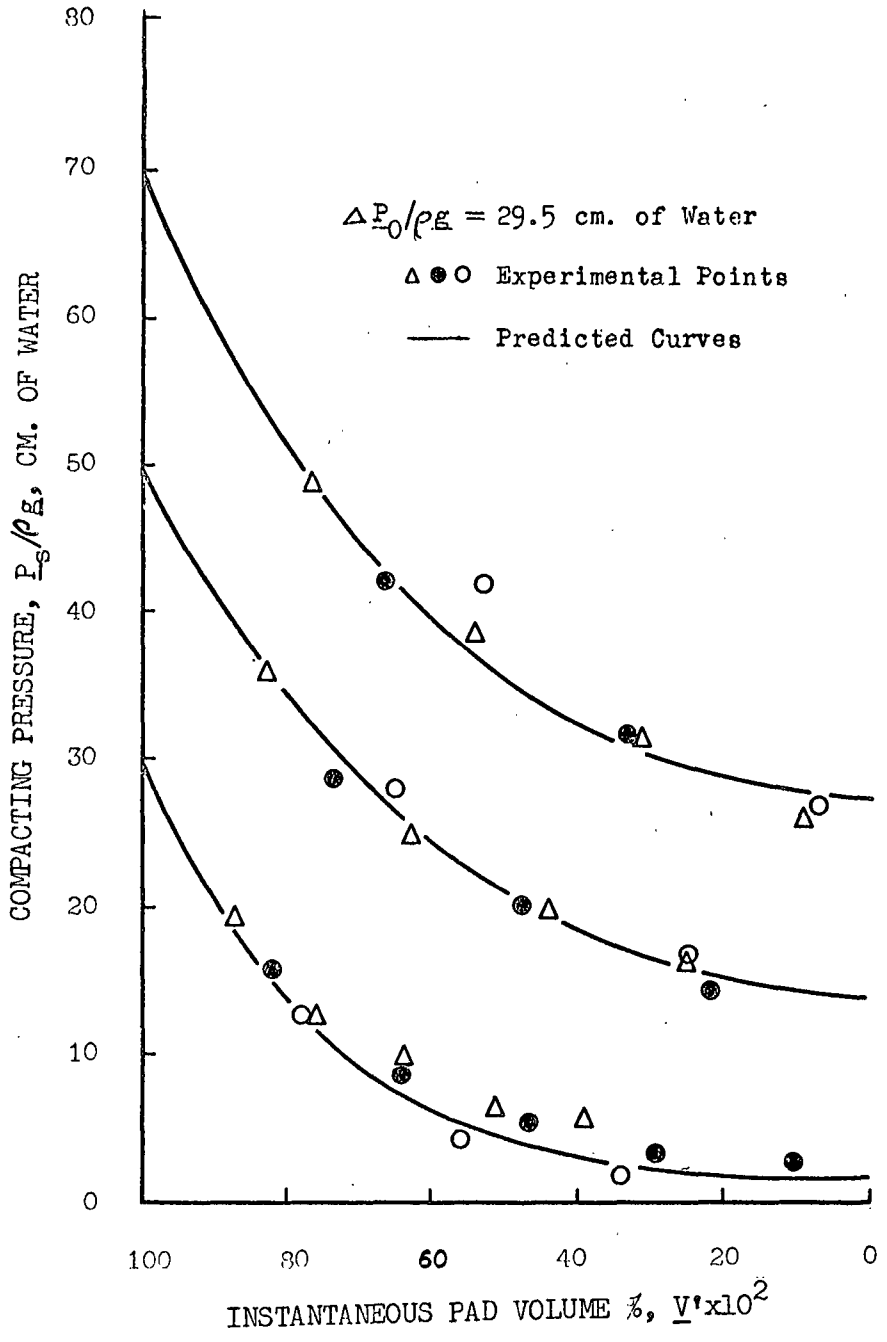

Figure 13 Internal Pressure Distributions, Compacting Pressure versus Instantaneous Pad Volume %

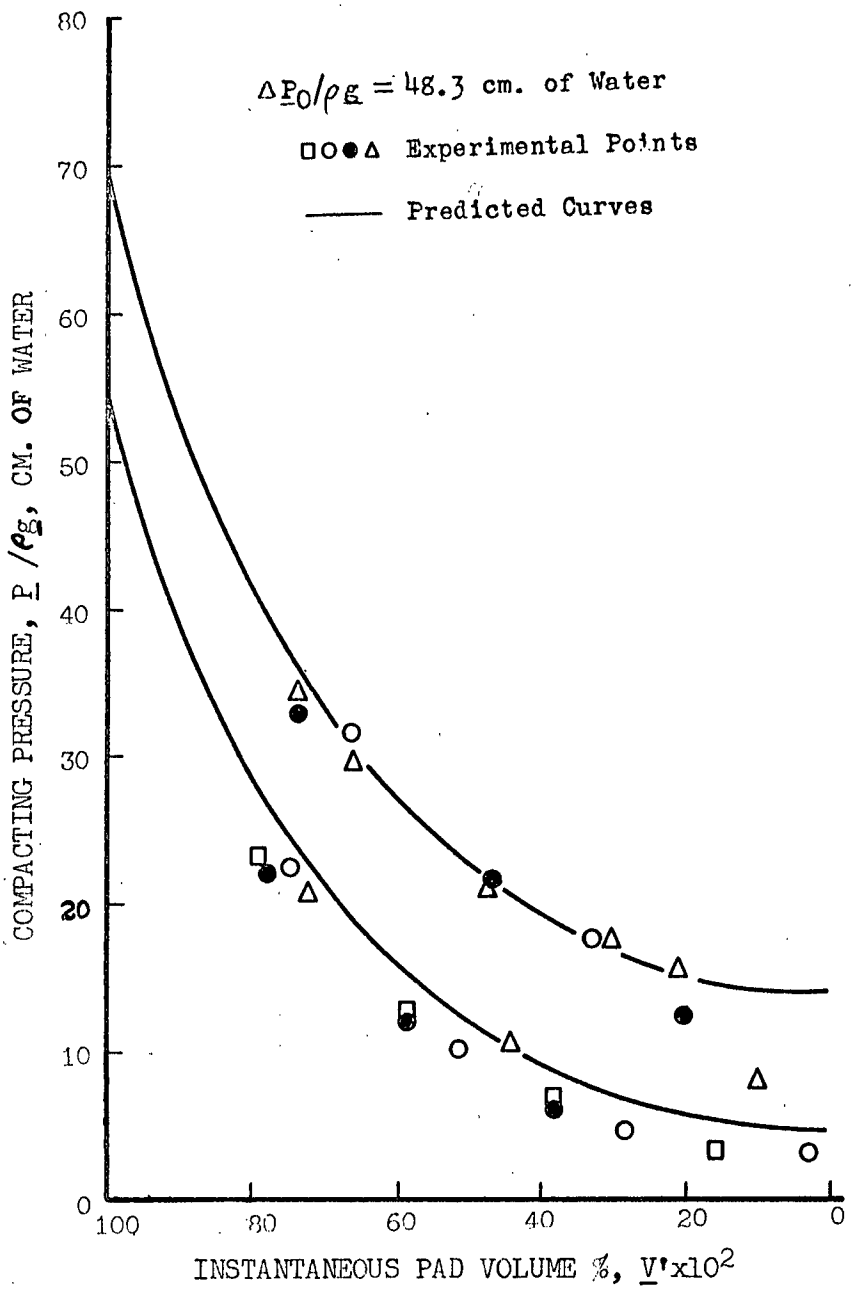

Figure 14 Internal Pressure Distributions, Compacting Pressure versus Instantaneous Pad Volume %

Error Considerations

The discussion of error in connection with the over-all pressure-drop data applies here in general to the internal-pressure-distribution data. In addition, however, there are four possible sources of error particularly important in the pressure-distribution determinations. These are:

1. The pressure taps have a radius of 3/32-in., and this introduced an uncertainty as to the position to be assigned to the pressure recorded.

2. There was a net flow of water out of the taps into the pad during the course of a run, which could have upset the pad to some extent.

3. There could have been a wall effect.

4. The pads might not have been uniform.

The first source of uncertainty, arising from the use of a discrete top cross section to measure a point pressure, is not amenable to close measurement or calculation. The uncertainty introduced is negligible, however, through the greater part of most thickenings. The tap radius of 3/32 in. is only 3% of the height of a three-inch pad, or 10% of a one-inch pad, which is the thinnest used. These are probably maximum limits, as the tap is measuring an average pressure across its face, which makes the center the best estimate.

The second source of error was the flow of water out of the manometers into the pad. This flow should tend to lower the pressure recorded by the manometers. However, since the total flow out of any of the manometers during an actual run was only 0.3 cc., and this was spread out over from 13 to 100 seconds, it is felt that this effect could be safely neglected.

The third possible source of error was the disturbing effect of the wall on the fiber and water flow in its immediate vicinity. Since the flow velocities involved were very small, 0.1 to 0.2 cm./sec., it is to be expected that this should not be an important factor.

The fourth source of error was in the nonuniformity of the pad itself, so that a pressure at one tap might not be a true indication of the pressure at the same height at other points in the pad. To check this, pressures were measured throughout each pressure-distribution run at two taps which were at the same height above the septum, but displaced 120° around the tube from one another. The variation between the two readings was never more than about one cm. of water, which was about the limit of the accuracy of the method employed to read the manometers. That would indicate that the pads were very nearly uniform in cross section.

SUMMARY AND CONCLUSIONS

An operation called thickening was postulated to play an intermediate step in the removal of fluid from a slurry of a material which forms a compressible mat. This operation starts when the last of the free slurry disappears and only a pad is left, and ends when a second fluid, such as air breaks into the pad.

The essential characteristics of this operation are:

1. The fluid movement is <u>out</u> of the pad and not through it.

2. The entire pressure drop across the bed, or applied force, is not available as a fluid driving force. On the contrary, part is counteracted by the mechanical strength of the bed itself.

3. The volume of the bed steadily decreases throughout this operation.

From these considerations, the concept of point specific filtration resistance, and a modification of D'Arcy's law, a mechanism for the operation was postulated, and a mathematical statement of this mechanism developed. The mechanism and especially its mathematical statement are closely analogous to the case of unsteady-state heat flow in a homogeneous body with temperature-dependent conductivity and heat capacity.

The mathematical statement was further developed for the special case of constant rate thickenings which are continuations of constant-rate filtrations or permeations. This predicted that the course of any such thickening expressed as over-all pressure drop as a function of the pad volume fraction removed and the internal pressure distribution as a function of the mass or volume fraction of the pad are dependent only upon the material used and the original pressure drop across the pad at the

start of the thickening. A method of iterative numerical integration of a transformed form of the equation was used to calculate the course of thickenings based solely on the proposed theory and the compressibility and point specific filtration resistance of the pulp.

An apparatus was constructed with which it was possible to run constant-rate filtrations on dilute pulp slurries to determine the specific filtration resistance of the pulp. On the same apparatus it was possible to form pulp pads, and conduct constant-rate thickening runs on these pads by sealing off the top of the pad with a low-friction impermeable piston. The internal pressure distribution on a time and volume basis was measured by means of side-wall taps connected to mercury manometers which were photographed along with a clock.

A series of constant-rate thickenings were run in which the pad weight and flow rate were varied over a twofold range, and the initial pressure drops varied over a threefold range. The over-all pressure drops were determined as a function of time or pad volume-fraction removed, and agreed well with the curves predicted on the basis of the postulated mechanism. Internal pressure distributions were also determined over these ranges and also agreed with the predicted distributions within a few per cent. The sources of error in the experimental and theoretical results were evaluated and found not to affect the conclusions.

From the success of the proposed mechanism for the postulated operation in independently predicting the results of the thickening runs, it is established that there is such an operation as thickening, and that the proposed mechanism of this operation must be essentially correct in all

major respects. It is to be noted, however, that there are limitations to the equations developed. These are:

1. Streamline flow must be maintained within the pad.

2. There must be only a negligible difference in the creep effects in the compression of the pulp pad during the thickening and in the compressibility and resistance determinations.

3. The septum resistance must be negligible or a suitable correction made.

4. No gross irregularities may exist in the pad. That is, the pad must be of uniform basis weight, but small-scale flocculation is allowable.

LITERATURE CITED

1. Muskat, M. The flow of homogeneous fluids through porous media. p. 71. New York, McGraw-Hill Book Co., 1937.

2. Brownell, L. E., and Katz, D. L., Chem. Eng. Progr. 43, no. 10:537-44 (Oct., 1947); no. 11:601-12(Nov., 1947); no. 12:703-12(Dec., 1947).

3. Silverblatt, C. E., and Dahlstrom, D. A., Ind. Eng. Chem. 46, no. 6: 1201-7(June, 1954).

4. Dombrowski, H. S., and Brownell, L. E., Ind. Eng. Chem., 46, no. 6: 1207-19(June, 1954).

5. Ingmanson, W. L. An investigation of the mechanism of water removal from pulp slurries. Doctor's Dissertation. Appleton, Wis., The Institute of Paper Chemistry, 1951. 119 p.

6. Ingmanson, W. L., Tappi 35, no. 10:439-48(Oct., 1952).

7. Ingmanson, W. L., Chem. Eng. Progr. 49, no. 11:577-84(Nov., 1953).

8. Ingmanson, W. L., and Whitney, R. P., Tappi 37, no. 11:523-34(Nov., 1954).

9. Preston, J. M., and Nimkar, M. V., J. Text. Inst. 43:T402(1952).

10. Christensen, S. N., and Barkas, W. W., Trans. Faraday Soc. 51, Part I:130-46(Jan., 1955).

11. Campbell, W. B., Pulp & Paper Mag. Can. 48, no. 2:103-9(1947).

12. Cowan, E., Pulp & Paper Mag. Can. 38:85-9(Convention, 1937).

13. Grace, H., Chem. Eng. Progr. 49, no. 6:303(June, 1953); 49, no. 7: 367(July, 1953).

14. Plunkett, R., Trans. Am. Soc. Mech. Eng. 73:605-8(July, 1951).

15. Ingmanson, W. L., and Whitney, R. P. Unpublished work, 1954.

16. Carman, P. C., Trans. Inst. Chem. Engrs.(London) 15:150-66(1937).

APPENDIX I

PRACTICAL IMPLICATIONS

The operation here called thickening is of some importance to the paper industry. It is involved in the formation of board and paper on fourdrinier and cylinder machines, and also in pressing operations. These are the major areas of application.

On fourdrinier machines, the importance of this operation is dependent mainly upon the weight of the sheet formed and the feed-stock consistency. On a tissue machine, using a very dilute stock and forming a very light sheet, this operation is of negligible importance, as air enters the sheet almost immediately after the disappearance of the last of the free slurry. On an insulating board machine, on the other hand, thickening is extremely important, as the feed-stock consistency may be over 1%, and thus there never would be a pad and slurry. The whole wet end is thus in thickening, from the slice down to the couch, if no air is drawn into the sheet on the boxes.

On intermediate weights on fourdrinier machines, the regime of thickening is of intermediate importance. It extends roughly from the first "dry" line to the second "dry" line, which normally centers around the last table rolls and the first suction boxes.

The pressing of any sheet which does not contain appreciable quantities of air should conform to the thickening theory. However, in nip pressing the flow is two-dimensional in a plane perpendicular to the plane of the sheet and the nip line. Thus, the development would have to be expanded by one dimension.

It should be noted that it is rare that a commercial case of thickening should be exactly a constant-rate or constant-pressure process, although thickening over the suction boxes on a fourdrinier machine approximates constant pressure quite closely. However, this does not affect the applicability of the theory and equations, which are valid whatever the rate or pressure schedule followed. This assumes, of course, that the schedule is known.

APPENDIX II

SAMPLE CALCULATION

The purpose of this section is to elucidate the method of calculation of the course of a thickening. To accomplish this, the calculations leading up to the predicted over-all pressure drop curve given in Figure 8 and the internal pressure distributions for the same run shown in Figure 13 are illustrated and followed through. All formulae and relationships which have not already been presented will be derived, and the reasoning behind the various steps shown. This will facilitate both the application of these methods to other problems and the evaluation of these methods in this work.

All of the necessary data on the pulp used has been given in Tables III and IV, in the form of average specific resistance as a function of over-all frictional pressure drop and equilibrium pad concentration as a function of mechanical compacting pressure.

ITEM A Calculation of average specific filtration resistance as a function of frictional pressure drop.

From the data obtained in the constant-rate filtrations it is desired to obtain the average specific filtration resistance of the pulp as a function of the frictional pressure drop across the pad.

At any instant during a constant-rate filtration it is seen from Equation (2) that

$$\underline{R}_{av} = \underline{A}\,\Delta\underline{P}_f/\mu\underline{M}q.$$

However, if $\underline{c}_s$ is the fiber mass deposited in the pad per unit volume of filtrate, and θ is the total elapsed time since the start of filtration, it is seen that $\underline{M}$, the pad mass per unit area, is given by

$$\underline{M} = \underline{c}_s \underline{q}\theta/A.$$

Thus, $\underline{R}_{av}$ may be expressed as

$$\underline{R}_{av} = (\underline{A}^2/\mu \underline{c}_s \underline{q}^2)(\Delta \underline{P}_f/\theta).$$

Some of the experimental data for one of the filtration runs, number 75, is given as follows:

Initial water height in tube	52.70 cm.
Final slurry height in tube	79.85 cm.
Total filtration time	557.8 sec.
Slurry temperature	23.0°C.
Volumetric flow rate	53.4 cc./sec.
Final pad weight	3.7273 g.
Partial filtration tube	424.0 sec.
Instantaneous pressure drop	51.0 cm. water

The calculations are illustrated below.

1. The total volume of filtrate was (557.8)(53.4) or 29,800 cc.

2. The volume of slurry additionally remaining in the tube, i.e., that required to fill the tube from 52.70 to 79.85 cm. was 1,890 cc. from a tube volume calibration.

3. The total volume of slurry was thus 29,800 plus 1,890 or 31,690 cc.

4. The pad weight, 3.7273 g., divided by the total volume, 31,690 cc., gives $\underline{c}_s$, which was thus 1.174×10^{-4} g./cc.

5. Values may now be substituted into the equation just developed for the average specific filtration resistance to give

$\underline{R}_{av} = [(50)^2/(0.009360)(1.174 \times 10^{-4})(54.3)^2][\Delta P_f/\theta] = 0.796 \times 10^6(\Delta \underline{P}_f/\theta)$.

where 50 is $\underline{A}$, the cross-sectional area of the tube in sq. cm., and 0.009360 is μ, the viscosity of water at 23.0°C. in poises.

6. At a time θ of 424 seconds, the frictional pressure drop was 51 cm. of water or (51)(980)(0.998) dynes/sq. cm., where 980 is the acceleration due to gravity and 0.998 is the density of water. The average specific filtration resistance on a mass basis is then

$$\underline{R}_{av} = (0.796 \times 10^6)(51)(980)(0.998)/(424)$$
$$= 0.937 \times 10^8 \text{ cm./g.}$$

This may be repeated to obtain enough points to plot $\underline{R}_{av}$ as a function of the frictional pressure drop across the pad over the range of interest, giving the points in Table III.

ITEM B Calculation of equilibrium pad concentration as a function of applied load.

It is desired to calculate the equilibrium (or pseudo-equilibrium) pad concentration as a function of the applied mechanical compacting force from the experimental pad height and load data. A set of these experimental data from run number 75 is given below.

Pad bottom position	58.52 cm.
Pad top position, uncorrected	59.28 cm.
Pad top correction	0.16 cm.
Pad top position, corrected	59.12 cm.
Net applied load	2005 g.
Pad weight, ovendry	3.7273 g.

The correction applied to the pad top reading is necessitated by

the fact that the cathetometer was not focused directly on the pad face, but on a point on the permeable piston 0.16 cm. above the face.

1. The pad concentration in this case is

$$\underline{c} = \underline{M}/\underline{h}\underline{A} = 3.7273/(59.12 - 58.52)(50)$$

$$= 0.1245 \text{ g./cc.}$$

2. The mechanical compacting load in this case is

$$\underline{P}_s = (2{,}005)(980)/50 = 39{,}300 \text{ dynes/sq. cm.}$$

$$\underline{P}_s/\rho\underline{g} = (2{,}005)/(50)(0.998) = 40.10 \text{ cm. water.}$$

ITEM C Calculation of point specific filtration resistance.

From the data on over-all specific resistance given in Table III, it is desired to calculate the point specific filtration resistance on a mass basis as a function of compacting pressure. It is first necessary to derive a working relationship between the point and average specific filtration resistances.

The average specific filtration resistance on a mass basis is exactly what its name implies. That is, it is defined and measured on the basis of the pressure drop across the whole pad in a permeation or filtration. Its definition is thus

$$\underline{R}_{av} = (1/\underline{M})\int_0^{\underline{M}} \underline{R}\, d\underline{m}, \tag{41}$$

where $\underline{M}$ is the top limit of the integration in terms of mass of pad solids per unit area, and $\underline{R}$ is the point specific resistance on a mass basis. Now, extend the limit of integration to $\underline{M} + d\underline{m}$. Then,

$$d\underline{R}_{av} = [1/(M + d\underline{m})]\int_0^{\underline{M} + d\underline{m}} \underline{R}\, d\underline{m} - (1/\underline{M})\int_0^{\underline{M}} \underline{R}\, d\underline{m}, \tag{42}$$

or

$$d\underline{R}_{av} = [1/(M + d\underline{m})]\left(\int_0^{\underline{M}} \underline{R}\, d\underline{m} + \underline{R}\, d\underline{m}\right) - (1/\underline{M})\int_0^{\underline{M}} \underline{R}\, d\underline{m}. \tag{43}$$

If reduced to the least common denominator and cleared, this gives

$$d\underline{R}_{av} = (1/\underline{M}^2)(\underline{RM} - \int_0^{\underline{M}} \underline{R}\, d\underline{m})d\underline{m}, \tag{44}$$

or using Equation (41), and rearranging,

$$\underline{R} = \underline{R}_{av} + \underline{M}\, d\underline{R}_{av}/d\underline{m}. \tag{45}$$

Expanding the derivative gives

$$\underline{R} = \underline{R}_{av} + (d\underline{R}_{av}/d\Delta\underline{P}_f)(d\Delta\underline{P}_f/d\underline{m}). \tag{46}$$

But Equation (31) may be rearranged to give

$$(d\Delta\underline{P}_f/d\underline{m}) = \underline{R}\Delta\underline{P}_f/\underline{M}\underline{R}_{av}, \tag{47}$$

which may be substituted into Equation (46) and rearranged to give

$$\underline{R} = \underline{R}_{av}/[1 - (\Delta\underline{P}_f/\underline{R}_{av})\ (d\underline{R}_{av}/d\Delta\underline{P}_f)]. \tag{48}$$

Using Equation (48), the point specific filtration resistance $\underline{R}$ may now be calculated as a function of compacting pressure from the average specific filtration resistance as a function of frictional pressure drop. As an example, the point specific resistance at 51 cm. water compacting pressure will be calculated. The necessary information follows.

$\Delta\underline{P}/\rho g.$ = 51 cm. of water.

$\underline{R}_{av} = 0.940 \times 10^8$ cm./g.

$d\underline{R}_{av}/d\Delta\underline{P}_f = 1.05 \times 10^3$ cm.^{3}/g. dyne.

Temperature = 25.4°C.

The derivative of the average specific filtration resistance with respect to the over-all frictional pressure drop ($d\underline{R}_{av}/d\Delta\underline{P}_f$) was obtained from a visual graphical differentiation of a plot of the data in Table III. Substituting this data into Equation (49) gives

$$\underline{R} = (0.940 \times 10^8)/[1 - (50)(980)(0.997)(1.05 \times 10^3)/(0.940 \times 10^8)]$$
$$= 2.06 \times 10^8 \text{ cm./g.},$$

where 980 is the acceleration due to gravity, g, cm./sec.^{2}, and 0.977 is the density of water at 25.4°C.

This calculation is then repeated to evaluate the point specific filtration resistance as a function of compacting load over the entire range of data in Table III.

ITEM D Evaluation of tau and $\underline{k}$.

To evaluate tau as a function of pressure and k, it is necessary only to know the point specific resistance as a function of compacting pressure, which was calculated as in item C, and the pressure limits of interest. The limits in this case were zero and one hundred cm. of water. Setting tau equal to pressure at these limits, as in Equation (19)

$$\tau_1 = 0(980)(0.997) = 0 \text{ dynes/sq. cm.}$$
$$\tau_2 = 100(980)(0.997) = 9{,}770 \text{ dynes/sq. cm.}$$

The constant $\underline{k}$ may now be calculated using Equation (20). Substitution of limits gives

$$\underline{k} = [1/(9{,}770 - 0)] \int_0^{9{,}770} d\underline{P}_s/\underline{R}. \qquad (49)$$

The integral is evaluated graphically by plotting the inverse specific filtration resistance from item A against compacting pressure, and measuring the area beneath the curve and between the limits. This area was $(68.93)(980)(0.997)(10^{-8})$ g. dynes/cm.^{3}, and so $\underline{k}$ is seen to be 0.689×10^{-8} g./cm.

Tau may be evaluated as a function of compacting pressure from Equation (21), which is now

$$\tau = (1/0.689 \times 10^{-8}) \int_0^{\underline{P}_s} d\underline{P}_s/\underline{R}.$$

The integral is graphically evaluated as in the calculation for $\underline{k}$, with the exception of different upper limits. At a compacting pressure of 50 cm. of water, the area under the curve between these limits was (50.85)(980)(0.977)(10^{-8}) g. dynes/cm.^{3}. Substituting into the equation gives

$$\tau = (50.85)(980)(0.977)(10^{-8})/(0.689 \times 10^{-8}).$$

$$= 72{,}200 \text{ dynes/sq. cm.}$$

τP_g. = 73.9 cm. of water.

This calculation is repeated at other values of compacting pressure, and the resulting tau values are plotted as a function of compacting pressure. This is now a complete conversion chart for the range of interest.

ITEM E Calculation of point compressibility.

In order to calculate the point compressibility of the pad over the desired range, using Equation (9), it is necessary to establish the apparent equilibrium pad concentration as a function of compacting load from a pressure of one hundred cm. of water down to a pressure of much less than one cm. of water. By the use of the permeable piston technique, this relationship was established over the range of ten to one hundred cm. of water, yielding the data presented in Table IV. It was necessary to obtain results indirectly for lower pressures, because of the weight of the permeable piston.

Equation (30) gives the volume of a pad undergoing permeation. By

introducing $\underline{M}'$, the reduced pad mass per unit area, this equation becomes

$$\underline{V}_o = \underline{AM} \int_0^1 d\underline{M}'/\underline{c}. \tag{50}$$

But substituting Equation (37) into this equation and rearranging gives

$$\underline{V}_o/\underline{AM} = (1/\Delta\tau_o) \int_0^{\Delta\tau_o} d\tau/\underline{c}. \tag{51}$$

Thus, the average volume of a pad per unit mass undergoing permeation at any given frictional pressure drop may be calculated from a knowledge only of the relationship between the point solids concentration $\underline{c}$ and the frictional pressure drop inside the pad, which may be converted to tau. This relationship is, however, known directly only for the range of ten to one hundred cm. of water.

The average volume per unit mass was determined experimentally for some pads undergoing permeation. It was found that the average volume per unit mass at an over-all frictional pressure drop of 33.5 cm. of water, or a tau drop of 60 cm. of water, was 22.7 cc./g. The reciprocal point concentration, or point volume per unit mass, is now plotted against tau from a pressure of 10 to 33.5 cm. of water, using the data in Table IV and the tau *versus* pressure conversion from item D. This plot is now extrapolated to zero pressure in such a way as to enclose an area under the curve between the limits such that the average volume per unit mass of this pad will agree with the experimental value of 22.7 cc./g.

This extrapolated curve of $1/\underline{c}$ *versus* tau was then checked by using it to compute the volume of other pads undergoing permeations at different over-all pressure drops. These volumes were also measured directly. The data on one such test is shown as follows:

Over-all pressure drop = 16.1 cm. of water

Over-all τ/ρg. drop = 41.5 cm. of water

= 40,500 dynes/sq. cm.

Pad mass = 18.8 g.

Tube area = 50 sq. cm.

Pad height = 11.0 cm.

Thus, the experimental value of pad volume is (50)(11.0) or 550 cc. But from the extrapolated plot, the integral in Equation (51) over this range is 1.177×10^6 dyne cm./g. Substituting this, and the appropriate experimental data, into Equation (51) will give a calculated value of the pad volume.

$$\underline{V}_o = [(50)(18.8/50)/40,500][1.177 \times 10^6]$$

$$= 546 \text{ cc.}$$

This, and other similar checks, showed that this guided extrapolation was sufficiently accurate for the purposes of this work.

This plot of reciprocal point concentration as a function of tau is now converted to a plot of reciprocal point concentration versus mechanical compacting pressure from the conversion chart prepared as in item D. This plot is now visually graphically differentiated to give the derivative $\partial(1/\underline{c})/\partial \underline{P}_s$, which is the point compressibility $\underline{Y}$ of the pad material. Thus $\underline{Y}$ was established over the entire range of interest in the system, which was zero to one hundred cm. of water pressure.

ITEM F Evaluation of "BYR" as a function of tau.

Equation (34) is the form of the equation which is to be used in the

final calculation of the course of a particular thickening run. This is, of course, a constant-rate thickening proceeding from a permeation at the same volumetric flow rate. The first necessary step in the solution is to establish the term "BYR" in this equation as a function of tau for the particular thickening of concern.

Experimental Data

Pad weight = 18.8 g.

Flow rate = 7.90 cc./sec.

Temp. = 25.4°C.

Viscosity = 0.00885 poises

Tube area = 50 sq. cm.

The over-all pressure drop across the pad during the permeation and at the start of thickening may be calculated by trial and error from Equation (2) using the average specific filtration data from Table III. For example:

Assume $\Delta P_f/\rho g$ = 48.3 cm. of water

Therefore, R_{av} = 0.930 x 10^8 cm./g.

But, $\Delta P_f/\rho g = \mu q M R_{av}/A\rho g$

Therefore, $P_f/\rho g$ = (7.90)(0.00885)(0.376)(0.915 x 10^8)/(50)(980)(0.997)

= 48.6 cm. of water

The final trial showed that the frictional pressure drop would be about 48.7 cm. of water. Converting to tau units, the over-all initial tau drop would be 71.5 cm. of water.

The total volume of the pad may be calculated as in item E. This calculation yielded a value for the average volume per unit mass of fiber

in the pad at a pressure drop of 48.6 cm. of water of 20.9 cc./g. Therefore, the original expected pad volume is (18.8)(20.9) or 392 cc.

From Equation (33), $\underline{B}$ may now be evaluated. It will be recalled that $\underline{B}$ is a constant, characteristic of the pad and flow rate only. In this case,

$$\underline{B} = \mu \underline{M}^2 \underline{q}/\underline{V}_o = (0.00885)(0.376)^2(7.90)/392$$
$$= 2.51 \times 10^{-5}.$$

Combining this value of $\underline{B}$ with the values of $\underline{R}$ as a function of tau from items C and D and the values of $\underline{Y}$ as a function of tau from items D and E, the composite term $\underline{BYR}$ is established as a function of tau. The reciprocal of this function is then plotted for use in the final iterative solution.

ITEM G The iterative solution of Equation (34).

To calculate the course of any thickening, Equation (34) was solved by a numerical iterative procedure similar to that used by Plunkett (13). A sample calculation of this sort will be given here for the experimental run for which the pertinent data has been presented in item F.

The reduced mass per unit area of the pad, $\underline{M}'$, is divided into equal sections of $\Delta \underline{M}'$ each. The reduced time is divided into steps of $\Delta(1-\underline{v})$. The function tau at the center of a section $i\Delta \underline{M}'$ down from the top of the pad and at a time $j\Delta(1-\underline{v})$ from the start of the thickening is designated $\tau_{i,j}$. Tau at the closed face, or top of the pad, is designated by the subscript "o", and at the open face, or septum side of the pad, by the subscript "w". Equation (34) may now be approximated by the difference equation

$$(\tau_{i+1,j} - 2\tau_{i,j} + \tau_{i-1,j})/(\Delta M')^2 = \underline{BYR}(\tau_{i,j+1} - \tau_{i,j})/\Delta(1 - \underline{v}), \quad (52)$$

or

$$\Delta\tau_i = [(\tau_{i+1,j} - \tau_{i,j}) - (\tau_{i,j} - \tau_{i-1,j})]\Delta(1 - \underline{v})/\underline{BYR}(\Delta M')^2. \quad (52a)$$

Now, let $\Delta M' = 0.25$ for the calculation in question. To determine the first boundary condition, tau as a function of M' at zero time, Equation (37) is used, remembering that tau is desired in the center of each mass segment, and the over-all tau drop across the pad is 71.5 cm. of water. Therefore,

$$\tau_{i,o}/\rho g = (i - 0.5)(0.25)(71.5) \text{ cm. of water.} \quad (53)$$

The second boundary condition is the tau gradient at the septum during the course of the thickening. From Equation (40) it may be seen that this gradient during the course of a constant-rate thickening is constant, and is thus given by

$$(\partial\tau/\partial M')_{M'=1} = \Delta\tau_o = 71.5\ (980)(0.998) \text{ dynes/sq. cm.}$$

However, in this solution, $\Delta M' = 0.25$, and thus $\Delta\tau$ at the septum will be constant at 17.9 cm. of water throughout the course of the thickening. Since the upper face is considered impermeable, that is, there is no flow across it, the tau gradient at that surface will be zero throughout the thickening.

Utilizing these relationships, and BYR as a function of tau as developed in item F, Equation (34) may be solved iteratively. In Table VI the first few steps of an iterative solution are shown. It must be born in mind that the value of $\Delta(1-\underline{v})$ must be varied (decreased) during the course of the solution in order that the composite term $\Delta(1-\underline{v})/\underline{BYR}(\Delta M')^2$ should always be less than unity, and generally in the neighborhood

of 0.5. This is necessary to prevent oscillation of the solution.

This table may be extended as far as is desired, but only as far as the term BYR has been established, of course. All of the tau values in this table may now be translated into pressures, and the pressures at the four mass points plotted against (1-$\underline{v}$). The instantaneous volume fraction $\underline{V}'$ corresponding to the mass fraction $\underline{M}'$ is now determined for each mass position as a function of (1-$\underline{v}$). Since all of the mass increments are equal, the volume of each mass increment is proportional only to the value of the reciprocal concentration (1/$\underline{c}$) corresponding to that pressure. This value is read from the developed data in item C. The equation used is

$$V'_i = [\sum_{0}^{i-1} (1/\underline{c}) + 0.5(1/\underline{c})_i]/[\sum_{0}^{n} (1/\underline{c})].$$

This is a difference approximation of the differential equation

$$\underline{V}'_{\underline{M}'} = [\int_0^{\underline{M}'} (1/\underline{c})d\underline{M}']/[\int_0^1 (1/\underline{c})d\underline{M}'].$$

Below are tabulated the steps in this operation for the sample iterative solution given above at the reduced time of 0.397.

	Position				
	i=w	i=4	i=3	i=2	i=1
$\tau/\rho g$., cm. of water	78.2	69.3	52.7	37.8	26.1
$\underline{P}/\rho g$., cm. of water	58.1	45.0	25.7	13.6	7.4
(1/$\underline{c}$), cc./g.		7.71	9.93	12.6	16.5
$\underline{V}'$, dimensionless		0.918	0.730	0.489	0.177

This calculation may be repeated at every step of the calculated run, yielding pressure as a function of reduced time, (1-$\underline{v}$), and position in the

TABLE VI

AN ITERATIVE SOLUTION OF THE PROPOSED THICKENING EQUATION

Reduced Time $(1-\underline{v})$	Caption	w	Pad Position* i=4	i=3	i=2	i=1
0.0	$\Delta(1-\underline{v})=0.0312$					
	$\tau_{i,o}$	71.5	62.6	44.7	26.8	8.94
	$(\tau_{i+1,j}-\tau_{i,j})$	17.9	17.9	17.9	17.9	0
	$(\tau_{i+1,j}-\tau_{i,j})-(\tau_{i,j}-\tau_{i-1,j})$		0	0	0	17.9
	$\Delta\tau_i$		0	0	0	0.8
0.0312	$\Delta(1-\underline{v})=0.0312$					
	$\tau_{i,j}$	71.5	62.6	44.7	26.8	9.7
	$(\tau_{i+1,j}-\tau_{i,j})$	17.9	17.9	17.9	17.1	0
	$(\tau_{i+1,j}-\tau_{i,j})-(\tau_{i,j}-\tau_{i-1,j})$		0	0	0.8	17.1
	$\Delta\tau_i$		0	0	0.2	0.9
0.0624	$\Delta(1-\underline{v})=0.0312$					
	$\tau_{i,j}$	71.5	62.6	44.7	27.0	10.6
	$(\tau_{i+1,j}-\tau_{i,j})$	17.9	17.9	17.7	16.4	0
	$(\tau_{i+1,j}-\tau_{i,j})-(\tau_{i,j}-\tau_{i-1,j})$		0	0.2	1.3	16.4
	$\Delta\tau_i$		0	0.1	0.3	0.9
0.0936	$\Delta(1-\underline{v})=0.0312$					
	$\tau_{i,j}$	71.5	62.6	44.8	27.3	11.5
	$(\tau_{i+1,j}-\tau_{i,j})$	17.9	17.8	17.5	15.8	0
	$(\tau_{i+1,j}-\tau_{i,j})-(\tau_{i,j}-\tau_{i-1,j})$		0.1	0.3	1.7	16.8
	$\Delta\tau_i$		0.1	0.2	0.4	1.0
0.1248	$\Delta(1-\underline{v})=0.0312$					
	$\tau_{i,j}$	71.6	62.7	45.0	27.7	12.5

* For convenience, tau units are cm. of water.

pad on a mass fraction basis, $\underline{M}'$, or on an instantaneous volume fraction basis, $\underline{V}'$.

Since $\underline{P}_{sw}$ is numerically equal to the over-all pressure drop across the pad, when it is plotted as a function of reduced time, $(1-\underline{v})$, it yields the predicted curve for over-all pressure drop as a function of reduced time, as is shown in Figure 8 in the section on experimental results.

To obtain the internal pressure distribution at the various values of the over-all pressure drop across the pad, the first plot is that already mentioned of the four mass point pressures and the over-all pressure drop as a function of reduced time, $(1-\underline{v})$. Then the instantaneous internal pad volume fractions, $\underline{V}'$, corresponding to these points are plotted as a function of the reduced time. At the desired over-all pressure drop the pressures at the four internal mass points are read off and the volume fractions corresponding to these points at this time read off the other plot at the same reduced time. This data may now be plotted as internal mechanical compacting stress $\underline{P}_s$, *versus* instantaneous pad volume fraction $\underline{V}'$, yielding predicted internal pressure distributions such as shown in the section of experimental results. It will be noted that $\underline{P}_s$ at any point in the pad is numerically equal to the pressure drop through the pad to that point. In the experimental setup used, it is the difference between the corrected hydrostatic pressure at that point and atmospheric.

ITEM H Experimental internal pressure distribution.

The experimental internal pressure data obtained was in the form of hydrostatic liquid pressure, as cm. of water below atmospheric, as a

function of pad volume in cc. above the septum and a function of time or reduced time. To compare with the predicted distributions, it was necessary to convert this to the same form as the predicted values, that is, to internal pressure as a function of instantaneous pad volume fraction and reduced time.

The instantaneous pad volume fraction at any pressure tap point a height "h" cm. above the septum at a reduced time of $(1-v)$ is seen to be given by

$$V' = 1 - hA/vV_o.$$

where it is recalled that A is the cross-sectional area of the pad and V_o is the original volume of the pad.

To compare predicted and actual values at a given over-all pressure drop, the pressures at the various wall taps and the septum tap are plotted as a function of reduced time. At the desired over-all pressure drop the pressures at the internal tap points are read off, and the reduced time is determined. Then V' is calculated by the above formula for each tap. This yields data for an experimental plot of internal pressure distribution which may be directly compared with the calculated internal pressure distribution.